Mutations in the S4 Region Isolate the Final Voltage-dependent Cooperative Step in Potassium Channel Activation

Jennifer L. Ledwell*‡ and Richard W. Aldrich*‡

From the *Department of Molecular and Cellular Physiology, and the ‡Howard Hughes Medical Institute, Stanford University, Stanford, California 94305

ABSTRACT Charged residues in the S4 transmembrane segment play a key role in determining the sensitivity of voltage-gated ion channels to changes in voltage across the cell membrane. However, cooperative interactions between subunits also affect the voltage dependence of channel opening, and these interactions can be altered by making substitutions at uncharged residues in the S4 region. We have studied the activation of two mutant *Shaker* channels that have different S4 amino acid sequences, ILT (V369I, I372L, and S376T) and Shaw S4 (the S4 of *Drosophila* Shaw substituted into *Shaker*), and yet have very similar ionic current properties. Both mutations affect cooperativity, making a cooperative transition in the activation pathway rate limiting and shifting it to very positive voltages, but analysis of gating and ionic current recordings reveals that the ILT and Shaw S4 mutant channels have different activation pathways. Analysis of gating currents suggests that the dominant effect of the ILT mutation is to make the final cooperative transition to the open state of the channel rate limiting in an activation pathway that otherwise resembles that of *Shaker*. The charge movement associated with the final gating transition in ILT activation can be measured as an isolated component of charge movement in the voltage range of channel opening and accounts for 13% ($\sim$1.8 e_0) of the total charge moved in the ILT activation pathway. The remainder of the ILT gating charge (87%) moves at negative voltages, where channels do not open, and confirms the presence of *Shaker*-like conformational changes between closed states in the activation pathway. In contrast to ILT, the activation pathway of Shaw S4 seems to involve a single cooperative charge-moving step between a closed and an open state. We cannot detect any voltage-dependent transitions between closed states for Shaw S4. Restoring basic residues that are missing in Shaw S4 (R1, R2, and K7) rescues charge movement between closed states in the activation pathway, but does not alter the voltage dependence of the rate-limiting transition in activation.

KEY WORDS: gating • ion channel • patch clamp • *Shaker*

INTRODUCTION

Voltage-dependent ion channels respond to changes in the electric field across the cell membrane by undergoing conformational changes that open and close an ion-permeable pore. The voltage dependence of channel opening, or activation, is caused by rearrangement of charges within the channel protein associated with conformational changes, thereby making the rates of the conformational changes voltage dependent. The movement of charge within the channel can be detected as gating current (Schneider and Chandler; 1973; Armstrong and Bezanilla, 1974, 1977; Keynes and Rojas, 1974; Stühmer et al., 1991; Bezanilla et al., 1991, 1994; Schoppa et al., 1992; Perozo et al., 1994; Sigg et al., 1994; Sigworth, 1994; Stefani et al., 1994; Zagotta et al., 1994a; Sigg and Bezanilla, 1997; Schoppa and Sigworth, 1998a–c).

Address correspondence to Richard W. Aldrich, Department of Molecular and Cellular Physiology, and the Howard Hughes Medical Institute, Room B171 Beckman Center, Stanford University School of Medicine, Stanford, CA 94305-5345. Fax: 650-725-4463; E-mail: raldrich@leland.stanford.edu

Understanding the molecular mechanism of voltage-dependent gating is an important goal of ion channel biophysics. Voltage-dependent potassium channels are particularly attractive for structure–function studies because members of this family share considerable sequence similarity, but exhibit a wide range of gating behaviors. Also, functional voltage-dependent potassium channels can be expressed as homotetramers, and the symmetry of a homotetrameric protein is likely to be reflected in the gating process. Studies on *Shaker*, a voltage-dependent potassium channel cloned from *Drosophila*, have yielded many important insights into processes of activation. However, the ability to study the gating process in wild-type *Shaker* is limited by the fact that it is difficult to study individual transitions independently of one another because the rates and voltage dependences of most of the transitions in *Shaker* activation are too similar (Zagotta et al., 1994b). The ability to perturb the energies of gating transitions with site-directed mutations provides a means to dissect out steps in the gating pathway for study using electrophysiological methods.

The fourth transmembrane segment (S4) of voltage-gated cation channels has been proposed to function

as a voltage sensor because of its high charge density and the fact that it has been highly conserved among voltage-gated cation channels (Noda et al., 1986; Catterall, 1988; Durrell and Guy, 1992). The sequence of the S4 is unusual, consisting of repeating basic residues at every third position, separated by neutral or hydrophobic residues (Noda et al., 1984; Salkoff et al., 1987; Tanabe et al., 1987, 1988; Papazian et al., 1987; Tempel et al., 1988; Baumann et al., 1988; Ellis et al., 1988; Kayano et al., 1988).

The results of several different lines of experimentation provide strong evidence for a role of the S4 in sensing voltage. Consistent with this hypothesis, it has been shown that mutations that neutralize S4 charged residues can decrease the amount of charge moved per channel during activation of *Shaker* (Aggarwal and MacKinnon, 1996; Seoh et al., 1996) and can decrease the voltage sensitivity of channel opening in voltage-gated sodium and potassium channels (Stühmer et al., 1989; Papazian et al., 1991; Liman et al., 1991). Further, studies on skeletal muscle sodium channels and *Shaker* potassium channels have demonstrated that the S4 region "moves" during activation by showing that the accessibility of some S4 residues to externally and internally applied chemical modifying reagents can be manipulated by holding the channel in open or closed conformations (Yang and Horn, 1995; Yang et al., 1996; Larsson et al., 1996; Mannuzzu et al., 1996; Yusaf et al., 1996; Baker et al., 1998).

However, the results of recent experiments suggest that the S4 is not only involved in sensing voltage during activation, but also in mediating cooperative interactions between channel subunits (Smith-Maxwell et al., 1998a,b). Substitution of the S4 segment from the *Drosophila* channel *Shaw* into *Shaker* causes a dramatic decrease in the voltage dependence of channel opening and makes the time course of activation slow and single exponential (Smith-Maxwell et al., 1998a). The slow, single-exponential gating kinetics suggest that the Shaw S4 mutation alters activation gating by slowing a cooperative transition in the activation pathway sufficiently to make it rate limiting. Smith-Maxwell et al. (1998a) also found that the gating of heterodimers with wild-type *Shaker* and chimeric Shaw S4 subunits can be predicted from properties of the homotetrameric channels only if it is assumed that the mutations alter cooperative transitions in the activation pathway rather than independent transitions.

Further, Smith-Maxwell et al. (1998b) found that the kinetic and voltage-dependent properties of the Shaw S4 ionic currents can be reproduced by introducing a subset of the substitutions present in the chimera into *Shaker*: V369I, I372L, S376T, to make the ILT mutant. The gating behavior of the ILT and Shaw S4 mutants can be accounted for by making the final cooperative transition rate limiting in a kinetic model of *Shaker* activation, without changing the rates or voltage dependences of any other transitions in the pathway (Smith-Maxwell et al., 1998a,b).

Cooperativity between subunits is a recurrent feature in the various kinetic models of potassium channel gating, but it can be implemented in any of a number of ways, including: a sequential mechanism in which the movement of each voltage sensor facilitates the movement of the next one (Tytgat and Hess, 1992), a cooperative stabilization of the open state (Zagotta et al., 1994b), and the presence of one or more highly cooperative or concerted transitions in the activation pathway (Schoppa et al., 1992; Sigworth, 1994; Bezanilla et al., 1994; Schoppa and Sigworth, 1998c). At present, little is known about the underlying conformational changes that produce the cooperativity that is observed in the activation of potassium channels.

In this paper, we investigate activation of the Shaw S4 chimera and ILT mutant at the level of gating currents to learn more about the role of the S4 in cooperativity and voltage sensing in the process of activation. Gating current recordings allow us to observe directly the charge movement associated with the voltage-dependent conformational changes that the channel undergoes in the activation pathway. Thus, gating current recordings from Shaw S4 and ILT channels can provide valuable insights into the nature of the cooperative conformational change and its position in the activation pathway and can reveal effects of the mutations on other transitions in the activation pathway that may be masked at the level of ionic currents by the presence of a rate-limiting transition.

MATERIALS AND METHODS

Molecular Biology and Terminology

All experiments were performed on a mutant form of *ShB* (Papazian et al., 1987; Kamb et al., 1987; Pongs et al., 1988), designated ShBΔ6–46, in which fast N-type inactivation was removed by deletion of amino acids 6–46 (Hoshi et al., 1990). This allowed us to study activation in isolation from the fast (N-type) inactivation process. ShBΔ6–46 still undergoes a relatively slow inactivation process (C-type inactivation), but the time constant for C-type inactivation (~1.5 s) is sufficiently slow that it does not interfere with measurement of activation parameters (Hoshi et al., 1991). ShBΔ6-46 cDNA was further modified by the introduction of a unique "silent" StuI restriction enzyme site 3′ to the S4 coding region, at amino acid positions 380–382. This modification, which does not alter the amino acid sequence, was made using the polymerase chain reaction method to generate a cassette that was inserted between two naturally occurring unique restriction enzyme sites within the *Shaker* cDNA, StyI and NsiI. In this paper, the term "*Shaker*" will always refer to the ShBΔ6–46 construct.

The Shaw S4 chimera and ILT mutant were constructed as described in Smith-Maxwell et al. (1998a,b). The Shaw S4:RRK mutant substitutes eight hydrophobic residues from the S4 of Shaw into *Shaker* (see Fig. 1). The Shaw S4:RRK mutation was made by

annealing sense and antisense oligonucleotides spanning the unique StyI and the silent StuI restriction enzyme sites in *Shaker*, and ligating the annealed oligos into *Shaker* digested with StyI and StuI restriction enzymes. The sequence of Shaw S4:RRK was verified by dideoxy termination sequencing.

For gating current experiments, expression levels were increased for ILT, Shaw S4, and Shaw S4:RRK constructs by subcloning into a high-expression *Shaker* vector obtained from Ligia Toro. The high-expression *Shaker* construct contained a pore mutation that has been reported to render the pore nonconducting (Perozo et al., 1993; but see DISCUSSION). The high-expression vector was used as a background to make high-expression conducting and nonconducting versions of ILT, Shaw S4, and Shaw S4:RRK. To generate the conducting versions of ILT and Shaw S4, DNA from the S4 mutant constructs was cut with BsiWI and SpeI restriction enzymes, generating a fragment that includes the mutant S4 and the wild-type *Shaker* pore. These DNA fragments were substituted for the corresponding BsiWI to SpeI fragment in the high-expression W434F *Shaker* construct. To generate nonconducting versions of ILT, Shaw S4, and Shaw S4:RRK, DNA from the S4 mutant constructs was cut with the BsiWI and NsiI restriction enzymes to generate a fragment that includes the mutant S4 region, but not the pore region of the channel. These DNA fragments were substituted for the corresponding BsiWI-NsiI fragment in the high-expression W434F *Shaker* construct.

To distinguish between constructs that contain a wild-type pore sequence and the pore sequence with the W434F mutation, we refer to the channels as "conducting" and "nonconducting," respectively.

Expression System

All channels were expressed in *Xenopus* oocytes by injection of G(5′)ppp(5′)G capped mRNA from the different channel constructs. mRNA was transcribed in vitro from linearized plasmid containing channel DNA constructs as described previously (Zagotta et al., 1989; Hoshi et al., 1990). For the original DNA constructs of *Shaker* and the S4 mutants, mRNA was transcribed with T7 RNA polymerase from a KpnI-linearized DNA template. For the high-expression conducting versions of ILT and Shaw S4 and for the nonconducting (W434F) version of ILT, Shaw S4, and Shaw S4:RRK, mRNA was transcribed with T7 RNA polymerase from an EcoRI-linearized DNA template. Recordings of macroscopic ionic currents typically were carried out 1–10 d after injection, whereas gating current recordings typically were carried out 14–28 d after injection.

Electrophysiology

All experiments were carried out at 20 ± 0.2°C.

Macroscopic ionic currents. Electrophysiological recordings of macroscopic ionic currents were carried out from excised membrane patches in the inside-out configuration (Hamill et al., 1981). The ionic current data for *Shaker*, Shaw S4, and ILT presented in Figs. 2 and 3 were taken from Smith-Maxwell et al. (1998a,b). For all other ionic current recordings presented in this paper, currents were recorded with an Axopatch 1B (Axon Instruments) patch clamp amplifier and low-pass filtered using an eight-pole Bessel filter (Frequency Devices, Inc.). The standard extracellular (pipette) solution used for these experiments contained (mM): 140 NaCl, 2 KCl, 6 $MgCl_2$, 5 HEPES (NaOH), pH 7.1. The standard intracellular solution (bath) contained (mM): 140 KCl, 11 EGTA, 10 HEPES (*N*-methylglucamine), pH 7.2. Ionic currents were digitized at 50–200 μs/point, depending on the channel kinetics. All data were filtered at 9 kHz unless otherwise stated. Details are stated in the figure legends. A Macintosh-based system with hardware interface from Instrutech Corp. and software from HEKA Electronik was used to generate pulses and digitize and store data. Patch pipettes were constructed from VWR borosilicate glass and had initial resistances of 0.4–0.8 MΩ. No series resistance compensation was used; however, the error due to uncompensated series resistance for this series of experiments was typically <2 mV (except for the gating current experiments on conducting channels in Fig. 7; see the legend of Fig. 7 and text for details). Linear leak and capacitative currents were subtracted with a P/4 protocol from a holding potential of −110 mV. A holding potential of −80 mV, followed by a 1-s prepulse to −100 mV was used before the test pulses.

Gating currents. Gating currents were measured either with a high performance cut-open oocyte voltage clamp (CA-1; Dagan Corp.) (Tagliatela et al., 1992) or with inside-out patches. The two different experimental procedures will be described separately.

In the cut-open oocyte clamp configuration, the oocytes were permeabilized by addition to the lower chamber of internal solution containing 0.3% saponin. Agar bridges with platinum iridium wire were filled with 1 M sodium methanesulfonic acid (NaMES). Microelectrodes were filled with 3 M KCl and had tip resistances of <1 MΩ. No series resistance compensation was used. Gating currents were digitized at 24 μs/point and filtered at 10 kHz. The internal recording solution included (mM): 110 KOH, 2 $MgCl_2$, 1 $CaCl_2$, 10 EGTA, 5 HEPES, adjusted to pH 7.1 with MES. The external recording solution included (mM): 110 NaOH, 2 KOH, 2 $MgCl_2$, 5 HEPES, adjusted to pH 7.2 with MES. Because *Shaker*, ILT, and Shaw S4:RRK gating currents activate in different voltage ranges, voltage and leak subtraction protocols had to be customized for each channel. For *Shaker*, ohmic capacitive and linear leak currents were substracted using either a +P/10 protocol from a holding voltage of +20 mV or a −P/5 protocol from a holding voltage of −120 mV. The leak-subtracted gating current records produced by the two procedures were not noticeably different. Since the gating currents of ILT and Shaw S4:RRK move over a much greater voltage range than those of *Shaker*, leak subtraction traces had to be taken in the voltage range of channel opening. Possible artifacts due to charge movement during leak pulses were minimized by choosing voltages for the leak subtraction where the kinetics of the channel are much slower (at least an order of magnitude) than the gating current signal of interest. For gating current recordings of nonconducting ILT, leak subtraction was performed using a +P/10 protocol from a holding voltage of +20 mV. For gating current recordings from nonconducting Shaw S4:RRK, we used a +P/5 leak subtraction protocol from a holding potential of +20 mV. For all cut-open oocyte clamp experiments, the oocyte membrane was held at −40 mV, and then stepped to −100 mV for 2 s before initiating more negative prepulse steps (prepulse voltages were −120 mV for *Shaker*, −140 mV for ILT, and −180 mV for Shaw S4:RRK), followed by test pulses. The properties of the gating currents did not change during the elapsed time of experiments. Details of voltage protocols, including prepulse voltages and durations, are given in the figure legends.

The inside-out patch clamp configuration was used to measure gating currents from nonconducting and conducting versions of ILT and Shaw S4 channels. Typical pipette resistances were 0.4–0.8 MΩ. The details of voltage protocols are given in the figure legends. Gating currents were digitized at 25 μs/point and filtered at 9 kHz. Standard patch clamp recording solutions (described above) were used, except at very positive voltages (greater than +100 mV). At voltages greater than +100 mV, patches containing nonconducting (W434F) ILT and Shaw S4 channels develop an outward ionic current that interferes with recording of gating

currents. The outward current can be eliminated by perfusing the intracellular side of the inside-out patches with a K^+-free solution containing (mM): 140 *N*-methylglucamine (NMG)–Cl, 11 EGTA, 10 HEPES, adjusted to pH 7.1 with NMG-OH. The outward current is probably caused by potassium conductance through the pores of the mutant *Shaker* channels, since the W434F *Shaker* mutant is not strictly "nonconducting," but has a very small open probability ($\sim 10^{-5}$) (Yang et al., 1997), and the size of the ionic current was found to correlate with the size of the gating currents in the patches. In most inside-out patch experiments on ILT gating currents, the holding potential was 0 mV. The holding potential can be held at −80, −40, or 0 mV without introducing any detectable changes in the amplitude or time course of gating currents in a given patch, at least over the time course of our experiments. A holding potential of 0 mV was used for Shaw S4 gating current experiments.

Analysis

For *Shaker*, conductance–voltage curves were constructed by calculation of the chord conductance (G_{chord}) from maximum currents (I_{max}) during the test pulse at several voltages (V) assuming a reversal potential (V_{rev}) of −80 mV: $G_{chord} = I_{max}/(V - V_{rev})$. For all other channel species, conductance–voltage curves were constructed from isochronal measurements of tail currents recorded at a fixed voltage after steps to voltages that activate the channels. Isochronal measurements were made between 0.2 and 1 ms after the end of the test pulse. Conductance–voltage curves were normalized to the maximum value for comparison between patches and between channel species. Conductance–voltage (*GV*)[1] curves were fit by a Boltzmann function of the form:

$$\frac{G}{G_{max}} = \left(\frac{1}{1 + e^{-zF(V - V_{1/2})/RT}}\right),$$

where G/G_{max} is the conductance normalized to the maximum value for each channel, $V_{1/2}$ is the voltage at which the channels are open half maximally, V is the voltage of the test pulse, z is the equivalent charge, F is the Faraday constant, R is the gas constant, and T is the absolute temperature. The slope factor is equal to RT/zF.

Activation kinetics were quantified by fitting the activation time course of macroscopic ionic currents with the following exponential function:

$$I(t) = A(1 - e^{(-t + d)/\tau}).$$

$I(t)$ is the current at time t, A is the scale factor for the fit, τ is the time constant, and d is the delay or amount of time required to shift the single exponential curve along the time axis to obtain an adequate fit of the activation time course. The time course of Shaw S4, ILT, and Shaw S4:RRK currents could be fit with this function from a beginning current level of between 1 and 5% up to the maximum current level. For *Shaker*, single exponential fits begin at between 20 and 50% of the maximum current to allow for the large sigmoidal delays characteristic of wild-type *Shaker* currents. Time constants for deactivation were obtained from fits of a single exponential to tail currents measured at negative membrane potentials. Tail currents were generally well fit by a single exponential function.

The voltage dependence of gating charge movement was determined by integrating the ON gating currents elicited by changes in membrane potential. Residual current at the end of test pulses was subtracted before ON gating currents were integrated. Gating charge was normalized to the maximum value to allow comparison of data across patches. To minimize artifacts caused by small drifts in the baseline, the ON gating currents were integrated over 12–30 ms, not the entire test pulse duration. Charge–voltage (*QV*) curves were fit with Boltzmann functions of the form:

$$\frac{Q}{Q_{max}} = \left(\frac{1}{1 + e^{-zF(V - V_{1/2})/RT}}\right).$$

The time constants of decay of the ON gating currents were measured by fitting a single-exponential function to the declining phase of the currents.

Modeling and Simulations

Model simulations were carried out as outlined in Zagotta et al. (1994b) using software developed in the Aldrich laboratory by Toshi Hoshi and Dorothy Perkins. Transitions between conformational states are assumed to obey time-homogeneous Markov processes. Voltage-dependent rate constants are assumed to be exponentially dependent on voltage.

RESULTS

Properties of the Ionic Currents of Shaker, Shaw S4, and ILT

The S4 sequences for *Shaker* and the mutant channels, Shaw S4 and ILT, are shown in Fig. 1. There are 11 amino acid differences between the Shaw S4 chimera and *Shaker*. Three of these occur at positions occupied by basic residues in *Shaker* (R1, R2, and K7), decreasing the charge content of the S4 from +7 in *Shaker* to +3 in the Shaw S4 chimera. The ILT mutant substitutes three noncharged residues (V369I, I372L, and S376T) from the Shaw S4 sequence into *Shaker*, so the nominal charge of the S4 region of the ILT is +7, like *Shaker*.

Despite the greater degree of similarity between the S4 regions of ILT and *Shaker*, the properties of the ionic currents of ILT are very similar to those of Shaw S4. The steady state, kinetic, and voltage-dependent prop-

	1	2	3	4	5	6	7	charge
Shaker	I	L	**R**	V	I	**R**	L	V	**R**	V	F	**R**	I	F	**K**	L	S	**R**	H	S	**K**	+7
Shaw S4	-	-	**E**	F	F	**S**	I	I	-	I	M	-	L	-	-	-	T	-	-	-	**S**	+3
ILT	-	-	-	-	-	-	-	-	-	I	-	-	L	-	-	-	T	-	-	-	-	+7
Shaw S4:RRK	-	-	-	F	F	-	I	I	-	I	M	-	L	-	-	-	T	-	-	-	-	+7

FIGURE 1. Comparison of S4 sequences for wild-type *Shaker* and mutant channels. Standard single letter code abbreviations are used to identify amino acids in the sequences. In the sequences of the mutants, dashes indicate amino acids that are identical to *Shaker*. The seven basic residues in *Shaker* are bold face and numbered. For wild-type *Shaker*, the first basic residue, R1, corresponds to amino acid position 362. The net charge of each S4 sequence is indicated in the "charge" column. Net charge was calculated assuming that arginine and lysine residues each contribute one positive charge, glutamate contributes one negative charge, and histidine is neutral.

[1]*Abbreviations used in this paper: GV*, conductance–voltage; *QV*, charge–voltage.

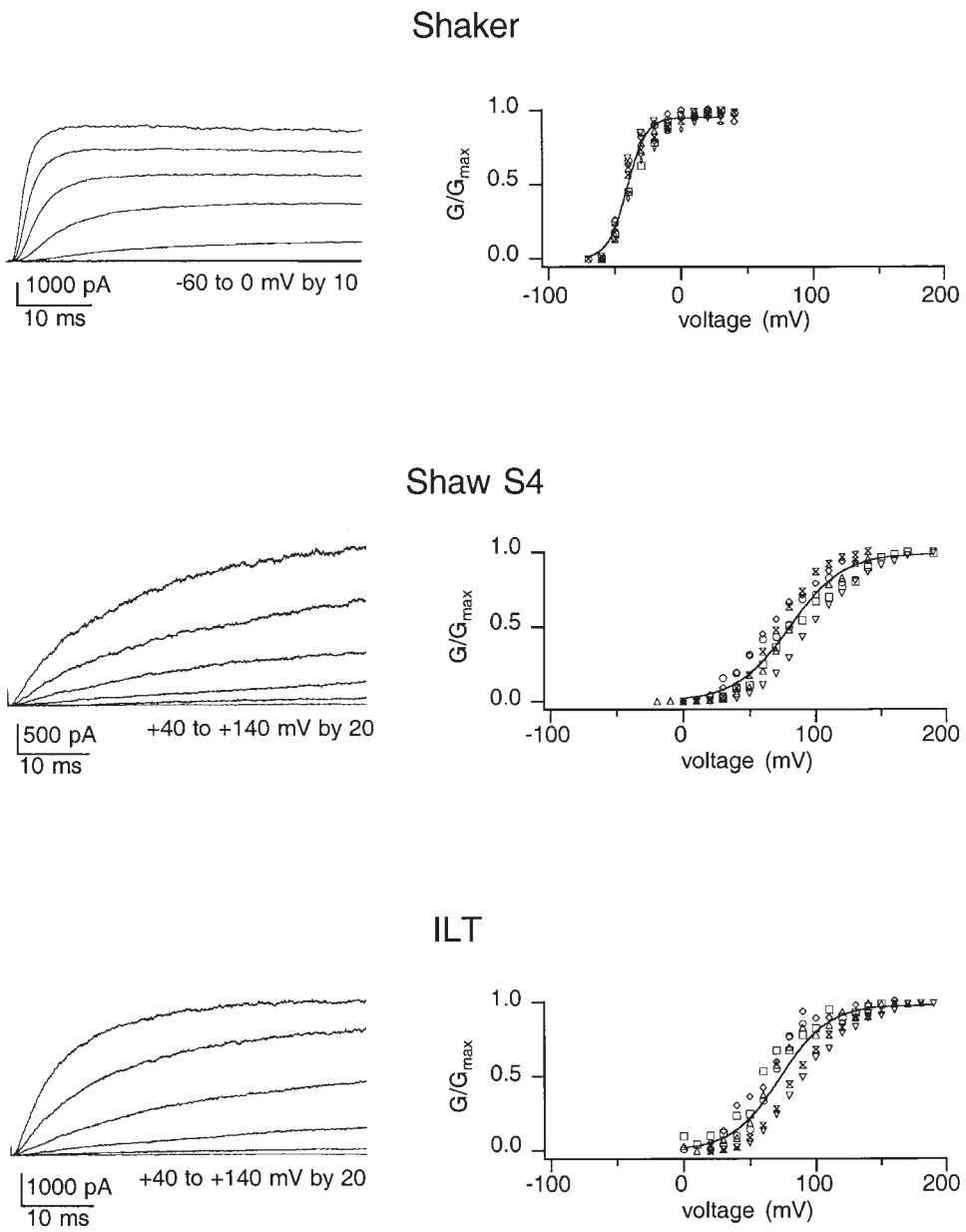

FIGURE 2. Macroscopic ionic currents and conductance–voltage relations for wild-type *Shaker* and mutant channels, Shaw S4, and ILT. (Left) Examples of currents from each channel construct recorded from inside-out patches. Currents were elicited by positive voltage steps to the voltages indicated, after a 1-s prepulse to −100 mV from a holding potential of −80 mV. (Right) Normalized conductance plotted as a function of voltage. Normalized conductance–voltage curves were constructed as described in MATERIALS AND METHODS. Each symbol represents a different experiment. The smooth curves through the data represent fits to the mean data for each channel with a Boltzmann function, as outlined in MATERIALS AND METHODS. The values from these fits are as follows, with n representing the number of experiments used to calculate each mean: *Shaker*: $V_{1/2} = -40.6$ mV, slope factor = 7.2 mV, $n = 8$; Shaw S4: $V_{1/2} = +80.1$ mV, slope factor = +20.4 mV, $n = 6$; ILT: $V_{1/2} = +73.0$ mV, slope factor = 18.3 mV, $n = 6$. *Shaker* currents were digitized every 50 μs and filtered at 2 kHz. Currents from ILT and Shaw S4 were digitized every 200 μs and filtered at 2 kHz. The conductance–voltage data for *Shaker*, Shaw S4, and ILT were taken from Fig. 2 of Smith-Maxwell et al. (1998b).

erties of the ionic currents are summarized in Figs. 2 and 3. A more thorough analysis of the ionic current behavior of Shaw S4 and ILT is presented in Smith-Maxwell et al. (1998a,b).

Fig. 2 shows ionic current traces and conductance–voltage curves of *Shaker*, Shaw S4, and ILT. The Shaw S4 and ILT mutations cause a large shift in the midpoint of the voltage dependence of channel opening (+120 mV) and a considerable decrease (2.7-fold) in the steepness of the conductance–voltage relation relative to *Shaker*. It is also apparent in Fig. 2 that the Shaw S4 and ILT mutations affect activation kinetics. The ionic current traces in Fig. 2 show that the ILT and Shaw S4 mutations greatly slow the overall rate of activation in the voltage range where channel opening probability is changing.

The effects of the Shaw S4 and ILT mutations on the time course of activation kinetics can be seen more readily in Fig. 3. The overall rate of activation of wild-type *Shaker* channels is fast, but the time course of activation is clearly sigmoidal and, at most voltages, there is a considerable delay after stepping to a new voltage before the current starts to rise (see also Zagotta et al., 1994a). This delay indicates that *Shaker* channels must undergo multiple transitions between closed states before opening. Further, the multiple transitions must have similar rates and voltage dependences because if one transition were rate limiting, it would dominate the time course of activation and produce a single-exponential time course. The fact that the early time course of wild-type *Shaker* activation cannot be fit with a single exponential function is illustrated clearly in Fig. 3,

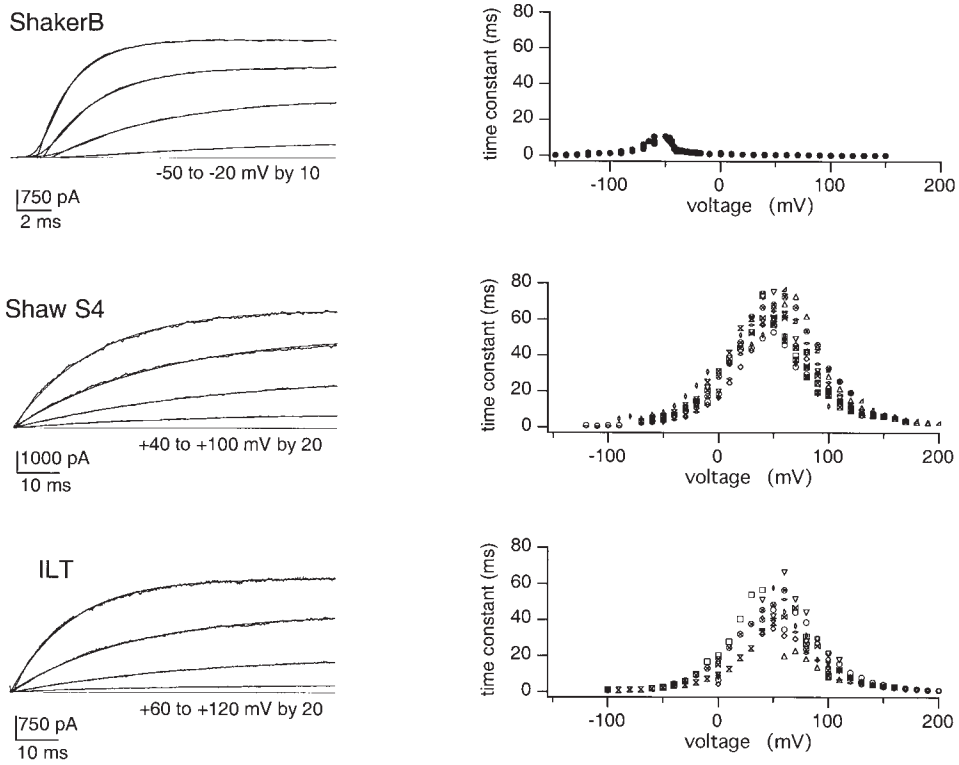

FIGURE 3. Gating kinetics for *Shaker*, the Shaw S4 chimera, and ILT mutant. (Left) Single exponential fits to the activation time course are shown superimposed on representative current traces for each channel. Note the different time scales. Currents were elicited by positive voltage steps to the voltages indicated, after 1-s prepulses to −100 mV from a holding potential of −80 mV. Current traces were fit with single-exponential functions as described in MATERIALS AND METHODS. The time course of Shaw S4 and ILT currents could be fit with a single-exponential function from a beginning current level of between 1 and 5% up to the maximum current level. For *Shaker*, single exponential fits begin at between 20 and 50% of the maximum current to allow for the large sigmoidal delays characteristic of wild-type *Shaker* currents. (Right) Time constants of activation and deactivation plotted as a function of voltage. Time constants were obtained from fits of single exponential functions to currents during channel opening and closing (see MATERIALS AND METHODS). Data from 10 patches with ILT currents and 14 patches with Shaw S4 currents are shown. ILT currents were digitized every 50 μs and filtered at 8 kHz. Shaw S4 currents were digitized every 200 μs and filtered at 2 kHz, or were digitized every 50 μs and filtered at 8 kHz. The time constants for *Shaker* and Shaw S4 were taken from Fig. 6 of Smith-Maxwell et al. (1998a) and for ILT were taken from Fig. 4 of Smith-Maxwell et al. (1998b).

where single exponential fits to the late phase of activation are shown superimposed on current traces.

The overall rate of activation of Shaw S4 and ILT channels is greatly slowed relative to *Shaker*, but, more importantly, the time course of activation of ionic currents of the mutants follows a single exponential time course over a wide voltage range. Analysis of the shape of the time course of activation of ionic currents is important because it can be used to distinguish mutations that primarily affect cooperativity from those that affect independent transitions. The slow, single-exponential gating kinetics of Shaw S4 and ILT suggest that these mutations alter activation gating by slowing a single transition in the activation pathway sufficiently to make it rate limiting (Smith-Maxwell et al., 1998a,b). Since the mutant channels presumably assemble into tetramers of four identical subunits (MacKinnon, 1991), the rate-limiting transition in Shaw S4 and ILT activation most likely arises from highly cooperative interactions between subunits. On the other hand, if a mutation slowed a transition that occurs independently in each of the four subunits of the channel, the time course of activation would be determined by four slow but identical transitions in the pathway to opening; as a result, the overall rate of activation would be slowed but the shape of the time course would be sigmoidal, not single-exponential (Smith-Maxwell et al., 1998a).

All of the properties of the ionic currents of the Shaw S4 and ILT mutants can be accounted for by making a final cooperative step in a kinetic model of *Shaker* rate limiting (Smith-Maxwell et al., 1998b). However, Smith-Maxwell et al. (1998b) found that the rate-limiting transition is so dominant in the activation process that the properties of the ionic currents of Shaw S4 and ILT can also be described well by a simpler two-state kinetic scheme in which the rate-limiting cooperative step is the only transition in the activation pathway. This finding suggests that effects of these mutations on other transitions in the activation pathway would be difficult to resolve at the level of ionic currents, but they should be visible at the level of gating currents.

Charge Movement between Closed States in ILT

The properties of the *Shaker* and ILT gating currents measured at negative voltages are summarized in Fig. 4. These measurements were made from nonconducting versions of *Shaker* and ILT, containing the mutation W434F (Perozo et al., 1993), in the cut-open oocyte clamp configuration.

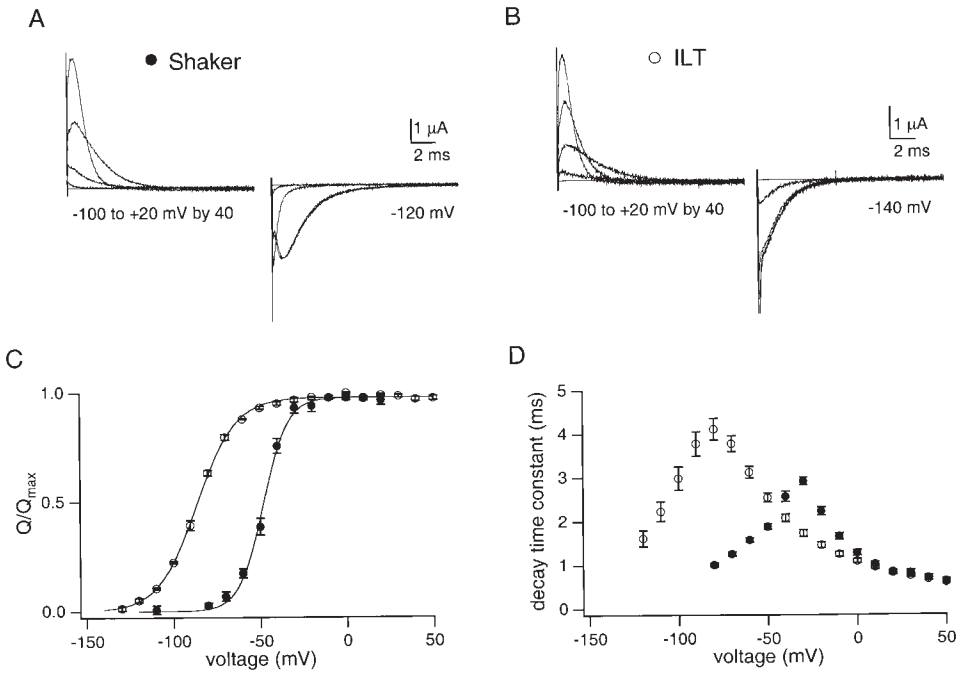

FIGURE 4. Gating currents from nonconducting *Shaker* and ILT channels recorded with cut-open oocyte clamp. (A) Representative *Shaker* gating current traces. ON gating currents were elicited in response to 50-ms steps to −100, −60, −20, and +20 mV from a 100-ms prepulse of −120 mV. OFF gating currents were elicited by 40-ms steps down to −120 mV after the test pulse. The first 10 ms of the ON and OFF gating current traces are shown. (B) Representative ILT gating current traces. ON gating currents were elicited in response to 50-ms steps to −100, −60, −20, and +20 mV from a 100-ms prepulse to −140 mV. OFF gating currents were elicited by 40-ms steps down to −140 mV after the test pulse. The first 10 ms of the ON and OFF gating current traces are shown. (C) Voltage dependence of charge movement. Normalized *QV* curves were constructed from the ON gating currents as described in MATERIALS AND METHODS. The smooth curves are fits of Boltzmann functions to the mean data as described in MATERIALS AND METHODS. The curve through the *Shaker* data represents a fit with $V_{1/2} = -48.24$ mV and the slope factor = 7.1 mV. The curve through the ILT data represents a fit with $V_{1/2} = -86.11$ mV and the slope factor = 11.3 mV. (D) Time constants of the decay of the ON gating currents plotted as a function of voltage. The declining phases of the ON gating currents were fitted with single exponential functions. The data were obtained from six experiments for *Shaker* and four experiments for ILT. Error bars in C and D represent the SEM.

The charge movement measured for ILT in the −140 to 0 mV voltage range must be associated with transitions between closed states because it moves in a voltage range where the channel does not open. The ILT mutation causes a negative shift (~38 mV) in the voltage dependence of this component of charge movement and reduces the steepness of the *QV* curve (Fig. 4 C) relative to wild-type *Shaker*. The movement of this component of gating charge saturates by −40 mV, which is 60 mV below the threshold of activation of ionic currents. There must be an additional component of charge movement in the voltage range of channel opening since the opening transition is voltage dependent. However, the gating charge that moves in the voltage range of channel opening could not be measured using the cut-open oocyte clamp technique because outward ionic currents develop at positive voltages and interfere with gating current recordings. The additional component of gating charge can be measured using inside-out patches (discussed below).

The ON gating currents of ILT strongly resemble those of *Shaker* in overall time course and relative voltage dependence, except that they activate in a more negative voltage range. Notably, both channels exhibit a rising phase in the ON gating currents, which is consistent with sequential steps in which a slower or less voltage-dependent transition is followed by a faster or more voltage-dependent transition (Zagotta et al., 1994b; Bezanilla et al., 1994; Schoppa and Sigworth, 1998a,c). The time constants measured from exponential fits to the decay phase of the ON gating currents are shifted to negative potentials compared with *Shaker* (Fig. 4 D). However, the amplitudes of the time constants of decay converge at voltages above 0 mV, consistent with the forward transitions in the activation pathways of *Shaker* and ILT possessing similar rates and voltage dependences.

The similarities observed between the ON gating currents of ILT and those of *Shaker* strongly suggest that *Shaker* and ILT channels have similar activation pathways. Considering the conservative nature of the individual amino acid substitutions introduced by the ILT mutation and the results from the analysis of ILT gating and ionic currents, it seems reasonable to propose that ILT channels undergo essentially the same conformational changes as wild-type *Shaker* during activation and that the ILT mutation simply alters the rates and equilibria of some transitions in the activation pathway.

An Additional Component of ILT Gating Charge in the Voltage Range of Channel Opening

The large separation in voltage range between the charge movement (Fig. 4) and the voltage-dependent channel opening (Fig. 2) of ILT indicates that there

must be an additional component of charge movement in the voltage range of channel opening. Measurements of the charge movement in the voltage range of channel opening will allow us to assess whether or not the rate-limiting cooperative step is the only charge-moving step in this voltage range. If the rate-limiting cooperative step is the only charge-moving gating transition in this voltage range, then: (a) the amount of gating charge measured in this voltage range should be in close agreement with the amount of charge associated with the rate-limiting cooperative transition as estimated from the voltage dependence of the rates of the opening and closing transitions, and (b) the time constants of decay of the ON gating currents in the voltage range of channel opening should have the same amplitude and voltage dependence as the time constants of activation of the ILT ionic currents.

Gating current traces from a typical experiment in inside-out patches are depicted in Fig. 5 A. We designed voltage protocols to measure separately the charge movement at negative voltages and the charge movement in the voltage range of channel opening. First, we measured charge movement in the −140 to 0 mV range, where the channel does not open, in inside-out patches. We then changed the holding potential of the membrane to 0 mV to allow charge movement between closed states to reach equilibrium. From a holding potential of 0 mV, we stepped briefly to high voltages (+100 to +180 mV), where channels open, to elicit charge movement associated specifically with the late transitions to the open state.

The gating currents measured at high voltages, where channels open, are much smaller than those measured in the same patch at negative voltages. Note that the scale bars for gating currents measured in the two different voltage ranges in Fig. 5 differ by an order of magnitude. Unfortunately, over much of the voltage range of interest, the ILT gating charge movement associated with the rate-limiting transition to opening cannot be measured because the amount of charge moved is very small and the time constant of gating charge movement is prohibitively slow (time constants for ILT ionic currents are shown in Fig. 3). Even in patches with very large numbers of channels, the gating charge signal is too small and slow to measure unless the membrane voltage is stepped to at least +130 mV. It is interesting to note that the gating currents at high voltages display a bit of a rising phase, a feature that could not be produced by a single transition. However, the presence of a rising phase should be interpreted with caution as it may be an artifact introduced by the leak subtraction procedure at these very high voltages rather than a true feature of the gating currents.

The voltage dependences of the total gating charge movement and of channel opening of ILT are shown plotted on the same graph in Fig. 5 B. The charge–voltage curve was constructed from the data obtained in the two different voltage ranges (−140 to 0 mV and 0 to +180 mV) by summing the amount of gating charge measured at high voltages with the amount of gating charge measured with steps to −20 mV, where the early component of gating charge movement has clearly saturated.

Gating current recordings detect the charge movement associated with all charge-moving transitions in the activation pathway. We can make use of this fact to determine whether or not the rate-limiting transition is the only charge-moving transition in the voltage range of channel opening. If the rate-limiting transition is the only gating transition that the ILT channel undergoes in the 0- to +180-mV voltage range, then the amount of gating charge measured in this voltage range should be in close agreement with the amount of charge estimated from the voltage dependence of the rates of the rate-limiting opening and closing transitions. On the other hand, if ILT undergoes additional charge-moving transitions that are not rate limiting in the 0- to +180-mV range, then the amount of gating charge measured in this voltage range must exceed the amount of charge estimated from the voltage dependences of the rates of the rate-limiting step.

The voltage dependence of the rates of the opening and closing transitions corresponds to equivalent charge values of 0.84 and 0.90 e_0, respectively, for a total of 1.74 e_0 predicted to move in the final opening step (Smith-Maxwell et al., 1998b). Thus, 1.74 e_0 represents a lower bound estimate for the amount of gating charge that must move per channel in this voltage range to account for the voltage dependence of the rate-limiting step, and additional voltage-dependent steps will increase the amount of the gating charge measured in the 0- to +180-mV range. Assuming that the total gating charge per channel is between 12.3 and 13.6 e_0 (Schoppa et al., 1992; Aggarwal and MacKinnon, 1994, 1996; Seoh et al., 1996), the proportion of gating charge moved in the rate-limiting transition corresponds to 13–14% of the total gating charge.

We determined the proportions of the total gating charge moved in the two voltage ranges of interest by measuring the charge moved by steps to voltages where the two components of charge were observed to saturate. The high-voltage component was measured with steps to +180 mV from a holding potential of 0 mV, and the low-voltage component was measured with steps to −20 mV from a prepulse potential of −140 mV. The total gating charge was taken to be the sum of these two values. We calculated that 13% (SEM, 0.9%; $n = 4$) of the total gating charge moved in the voltage range where channels open and 87% (SEM, 1.2%; $n = 4$) moved between −140 and −20 mV. Given that the

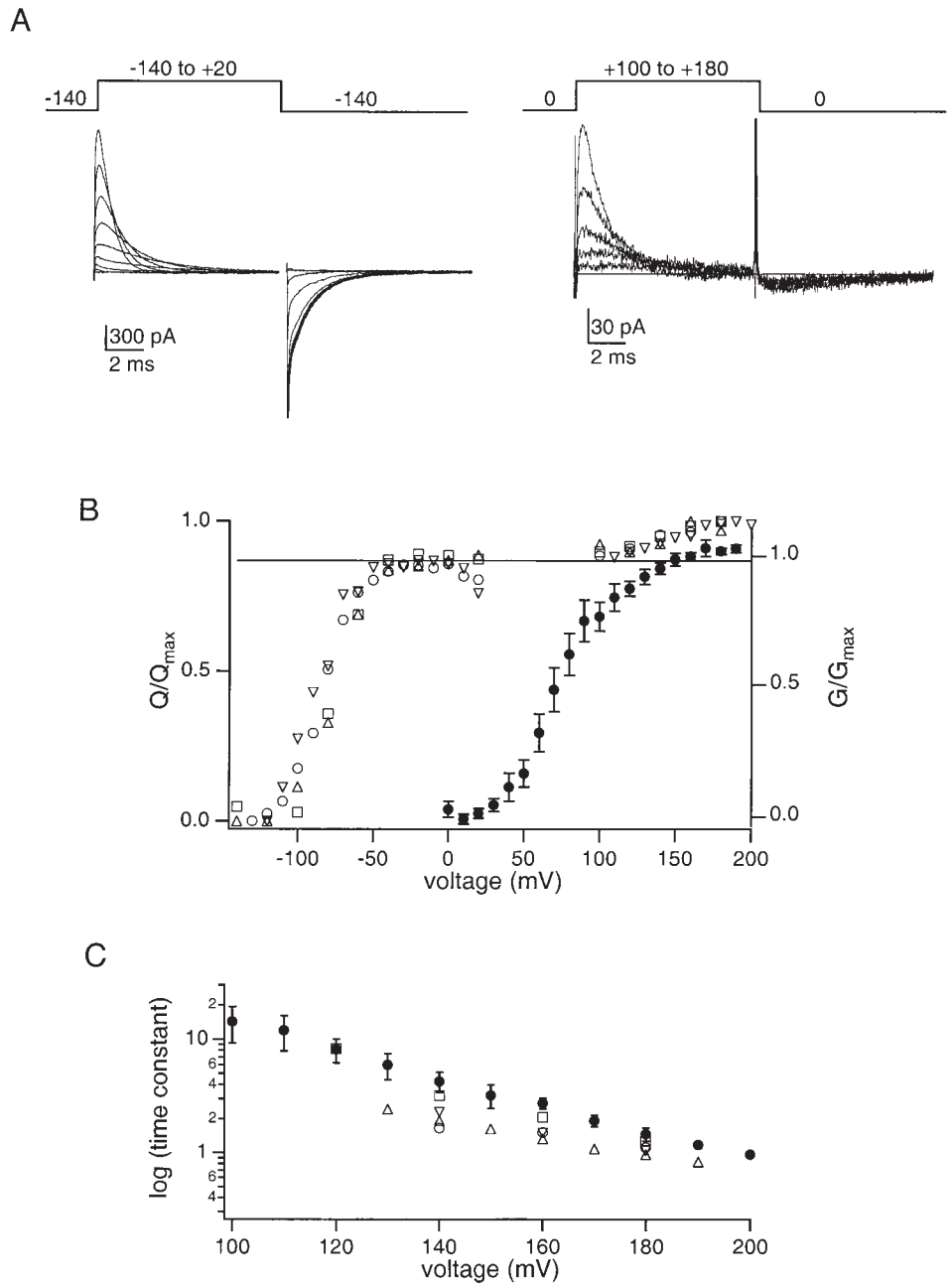

FIGURE 5. An additional component of ILT gating charge moves in the voltage range of channel opening. (A) Gating currents from nonconducting ILT channels recorded from inside-out patches. (Left) ON gating currents were elicited in response to 50-ms steps to −140 to +20 mV in increments of 20 mV after a 10-ms prepulse to −140 mV. OFF gating currents were elicited by steps down to −140 mV after the test pulse. The first 10 ms of the ON and OFF gating current traces are shown. (Right) The same patch was then held at 0 mV and ON gating currents at high voltages were elicited by 10-ms steps to +100 to +180 mV in 20-mV increments. (B) Voltage dependence of ON gating charge movement and channel opening. Normalized charge movement (*Q*V, open symbols) and mean conductance (*G*V, filled circles) for ILT are plotted against voltage. The scale for normalized charge movement is shown on the left and for normalized conductance is shown on the right. ON gating currents were elicited as described in A. Charge measurements from four different patches are shown, each symbol representing a different patch. The conductance data is the mean for six ILT experiments; error bars represent the SEM. The solid line indicates the saturation of charge movement at lower voltages at 0.87. This value was calculated from the average of the normalized charge values at −20 mV for all patches. Charge movement and conductance were calculated as outlined in MATERIALS AND METHODS. (C) Time constants of ON gating current decay (open symbols) and ionic current activation (filled symbols) as a function of voltage are shown. Time constants of ON gating current decay from four different patches are shown, each symbol representing a different patch. The time constants for ionic current represent the mean values calculated from seven patches; error bars represent SD. The ON gating currents were elicited as described in A. Time constants were measured as outlined in MATERIALS AND METHODS.

amount of charge moved in the activation pathway per wild-type *Shaker* channel has been estimated to be between 12.3 and 13.6 e_0 (Schoppa et al., 1992; Aggarwal and MacKinnon, 1996; Seoh et al., 1996), these proportions correspond to gating charge movements per channel of 1.6–1.8 e_0 in the 0- to +180-mV range and 10.7–11.8 e_0 in the −140- to −20-mV range. We assumed that the amount of gating charge moved per ILT channel is the same as for wild-type *Shaker* based on reports in the literature that mutations at neutral residues in the S4 and at the carboxy-terminal border of the S4 do not change the total amount of gating charge moved per channel (Schoppa et al., 1992; Aggarwal and MacKinnon, 1996).

The amount of gating charge that moves in the voltage range of channel opening, 1.6–1.8 e_0, is in very

close agreement with the value for equivalent charge associated with the rate-limiting transition, 1.74 e_0, estimated from analysis of the voltage dependence of the rates of channel opening and closing in ionic currents from Smith-Maxwell et al. (1998b). The agreement between these two independent determinations provides strong evidence that the only charge-moving step in the 0- to +180-mV range is the rate-limiting cooperative step that dominates the behavior of the ionic currents.

If the ILT gating charge movement at high voltages is associated with the rate-limiting cooperative transition between the final closed and open states, then the kinetics of the gating currents should be the same as the kinetics of the ionic currents. The voltage dependence of the time constants of decay of the ON gating currents at high voltages is shown plotted on the same graph as mean time constants of activation of ionic currents (Fig. 5 C). The gating current time constants have the same voltage dependence (slope) as the ionic current activation time constants, but the gating currents are noticeably faster than the ionic currents.

The discrepancy between the kinetics of the gating and ionic currents deviates from the prediction of a singe transition. However, it can be explained in terms of a voltage shift between the gating current and ionic current data (see DISCUSSION). If the voltage shift is corrected for, the amplitude and voltage dependence of the kinetics of the gating currents recorded in the voltage range of channel opening are consistent with those expected to accompany the gating charge movement during the rate-limiting cooperative transition that opens the ILT channel. Given that the amount of charge moved in this voltage range is in such close agreement with the equivalent charge measured for the rate-limiting cooperative transition based on the voltage dependence of the rates of ionic current activation and deactivation, it seems likely that the rate-limiting cooperative transition is the final charge-moving step in the activation pathway. Therefore, in spite of the voltage shift between the kinetics of the gating and ionic currents, it seems likely that the charge movement that we have measured corresponds to the charge moved in the rate-limiting cooperative step. The simplest interpretation of these findings is that the ILT mutation has uncovered the final voltage-dependent cooperative transition in the *Shaker* activation pathway by making it rate limiting.

The Activation Pathway of Shaw S4

The similar properties of the ionic currents of ILT and Shaw S4 imply that these two channels gate in the same way. However, the gating currents of Shaw S4 indicate that its activation pathway is fundamentally different from that of ILT.

The only gating charge that could be detected for nonconducting Shaw S4 channels moves at very positive voltages, in a voltage range where channels open (Fig. 6). We could not detect any Shaw S4 charge movement in the voltage range where most of the charge

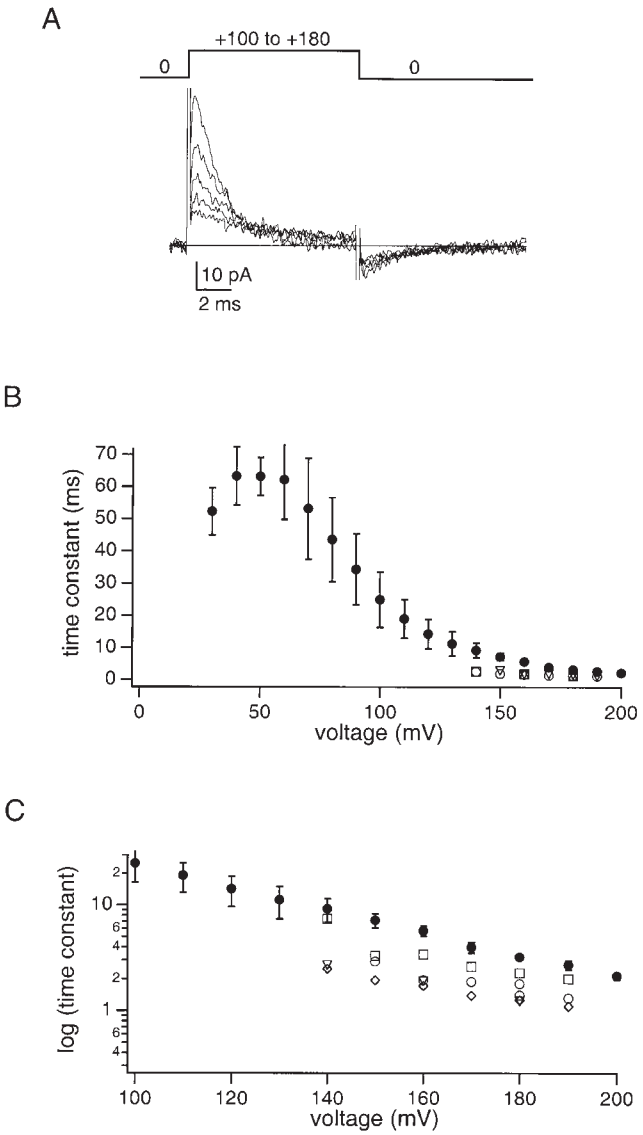

FIGURE 6. Gating currents from nonconducting Shaw S4 channels. (A) ON gating currents were elicited by steps to +100 to +180 mV in 20-mV increments from a holding voltage of 0 mV. For the purposes of presentation, the data were digitally filtered at 4 kHz. (B) Time constants of Shaw S4 ON gating current decay (open symbols) and ionic current activation (filled circles) as a function of voltage. Time constants of ON gating current decay from four different patches are shown, each symbol representing a different patch. The time constants for ionic current represent the mean values calculated from 14 patches; error bars represent the SD. Time constants were measured as outlined in MATERIALS AND METHODS. (C) A semi-logarithmic plot of the Shaw S4 ON gating current decay (open symbols) and ionic current activation time constants (filled circles). Error bars represent SD.

moves in the activation pathways of ILT and *Shaker*. The Shaw S4 gating currents strongly resemble the component of ILT gating currents recorded in the voltage range of channel opening (shown in Fig. 5 A) in shape and time course. As noted previously for ILT, the Shaw S4 gating currents cannot be measured over much of the voltage range of channel opening because the time constants of gating charge movement are prohibitively slow and the amount of charge moved is very small.

We cannot use the method applied to ILT to determine the amount of Shaw S4 gating charge moved at high voltages because of the absence of Shaw S4 gating charge at low voltages. However, we can measure time constants from currents elicited with steps to sufficiently positive voltages. The time constants of decay of the ON gating currents are shown plotted as a function of voltage on the same graph as time constants of activation of Shaw S4 ionic currents (Fig. 6, B and C). The kinetics of the gating currents are faster than the kinetics of the ionic currents but have a similar voltage dependence. The faster gating current kinetics correspond to a voltage shift of 20–25 mV relative to the ionic currents. This voltage shift is similar in magnitude to the voltage shift observed between the kinetics of the ionic and gating currents of ILT and probably occurs for similar reasons (see DISCUSSION).

The absence of charge movement between closed states in nonconducting Shaw S4 channels indicates that the chemical or steric properties of some of the substituted S4 residues may interfere with the normal conformational changes of the channel protein during gating. If the Shaw S4 gating charge detected in the voltage range of channel opening is associated with the rate-limiting cooperative transition, then the activation pathway of Shaw S4 moves as little as $\sim$1.8 e_0 per channel, or 0.45 e_0 per subunit. This value is less than expected considering the charge-changing substitutions in the S4 region of Shaw S4. While there are three charge-changing substitutions between the S4 of Shaw S4 and *Shaker*, only two of these substitutions occur at residues that have been shown to contribute to the gating charge of the channel (Aggarwal and MacKinnon, 1996; Seoh et al., 1996). With eight charge-moving residues per tetrameric channel protein remaining (i.e., two charge-moving residues per subunit), we would expect to see some charge movement between closed states in addition to the 1.8 e_0 per channel moved during the last cooperative transition.

It is also possible that the S4 mutations might interact with the pore mutation, W434F, to produce an anomalous gating phenotype. To address this possibility, we performed a series of gating current experiments with conducting ILT and Shaw S4 channels. In these experiments, we also extended the voltage range of investigation down to −240 mV in an attempt to measure Shaw S4 gating currents.

We selected inside-out patches that expressed very high levels of conducting channels and measured the amount of ionic current elicited by steps to +100 mV, then we tried to detect gating currents in the same patch in the −140 to 0 mV range, where most of the charge moves in the ILT activation pathway. A representative experiment for each channel is shown in Fig. 7. In patches expressing ILT channels, we were able to detect robust gating currents with steps to −140 to 0 mV in every patch that had at least 3.7 nA of ionic cur-

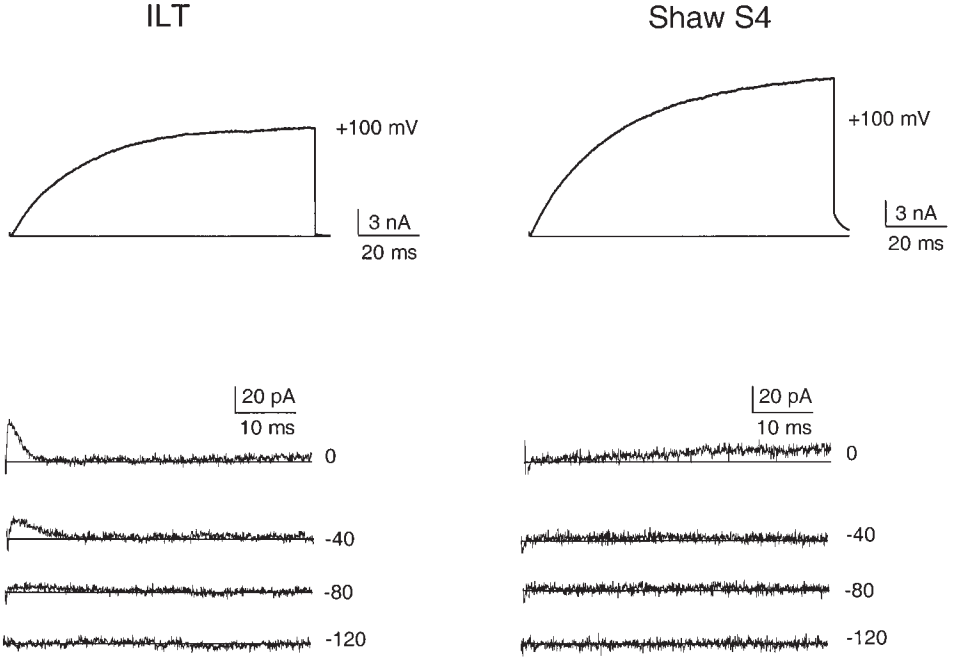

FIGURE 7. Gating currents in conducting ILT and Shaw S4 channels. (A) Macroscopic ionic currents (top) were elicited by steps to +100 from −140 mV, and then gating currents (bottom) were elicited from the same patches by steps to −120 through 0 mV in 40-mV increments from a prepulse to −140 mV. The ionic currents and the gating currents are displayed using different scales. The results of similar experiments on many patches are summarized in Table I.

rent at +100 mV. In patches expressing Shaw S4 channels, we were not able to detect any gating currents in the voltage range of −200 to 0 mV, even though we biased our experiments towards having more ionic current at +100 mV (i.e., more channels per patch) in the Shaw S4 experiments than the ILT experiments. For 6/11 patches of Shaw S4, we extended the voltage range of investigation with steps down to −240 mV (patches could not withstand more negative pulses), but we still did not detect gating currents in any patches expressing Shaw S4.

The results of similar experiments on many patches are tabulated in Table I. To interpret data across patches that had different numbers of channels, we normalized the data by calculating the ratio of gating charge at 0 mV to ionic current at +100 mV. The scatter in the q/K^+ current data is probably due to series resistance error introduced by the very large ionic currents that were measured. The accuracy of measurements of current at +100 mV would be quite sensitive to series resistance errors because the probability of opening is still changing (see Fig. 2). However, the direction of the series resistance error would cause us to underestimate systematically the true amount of ionic current at +100 mV, which in turn would cause us to overestimate the amount of gating charge moved relative to the true amount of ionic current. Our interpretation of these experiments would not be compromised by systematically underestimating the amount of ionic current at +100 mV.

As in the case of ILT, the discrepancy between the kinetics of the gating and the ionic currents of Shaw S4 can be explained readily in terms of a voltage shift, the possible causes of which will be presented in the DISCUSSION. If the voltage shift is corrected for, the amplitude and voltage dependence of the kinetics of the gating currents recorded in the voltage range of channel opening are consistent with those expected to accompany the gating charge movement during the rate-limiting cooperative transition that opens the Shaw S4 channel. Therefore, it seems likely that the charge movement that we have measured corresponds to the charge moved in the rate-limiting cooperative step. Further, it seems likely that the rate-limiting cooperative transition is the only charge-moving step in the activation pathway of Shaw S4, since we could not detect charge movement between closed states in the Shaw S4 mutant.

TABLE I

Comparison of Gating Charge to Ionic Current in the Same Patch

	K^+ current (nA)	q/K^+ current (fC/nA)	*n*
	mean ± SD	*mean ± SEM*	
ILT	9.8 ± 3.7	6.7 ± 1.3	11
Shaw S4	11.2 ± 4.8	0.00 ± 0.06	11

The mean K^+ current denotes the mean peak ionic current measured at +100 mV in patches for which the ratio of q/K^+ current was subsequently determined, and the standard deviation of the K^+ currents was included to indicate the range in the magnitude of ionic currents in these patches. q/K^+ current represents the ratio of gating charge (measured by integration at 0 mV) to peak ionic current (measured at +100 mV) in a given patch. SEM for q/K^+ current is included to indicate the patch-to-patch variability observed in the determination of q/K^+ current. Gating charge was measured in fC and ionic current was measured in nA. *n*, number of patches.

Although we could not detect gating charge movement between closed states in the Shaw S4 mutant using the methods described above, these methods do not prove the absence of such gating charge. Gating charge from a slow transition between closed states might escape detection using these methods. However, the presence of a slow transition between closed states should manifest itself in the sigmoidicity of the time course of activation. This possibility will be addressed experimentally in the following section.

Closed States in the ILT Activation Pathway Produce a "Cole-Moore Shift" that Is Absent in Shaw S4 Ionic Currents

The time course of activation of *Shaker* is fast, but at most voltages it is sigmoidal in shape and exhibits a large delay before the current starts to rise (discussed above; see also Zagotta et al., 1994a). This delay indicates that *Shaker* channels must undergo a number of voltage-dependent transitions between closed states before it can open. Depolarized holding voltages cause a decrease in the amount of delay in the time course of *Shaker* activation, presumably because channels now occupy states along the activation pathway that are closer to the open state of the channel (Zagotta et al., 1994a). A decrease in the delay in the time course of activation in response to depolarized holding potentials is often referred to as a Cole-Moore shift because the phenomenon was first observed in squid potassium channels by Cole and Moore (1960).

The presence of more closed states in the activation pathway of ILT than Shaw S4 can be seen on close investigation of the time course of activation of ionic currents. The properties of the ionic currents of Shaw S4 and ILT are very similar. However, at voltages above +140 mV, the time course of activation of ILT develops a very small but progressive increase in delay that is essentially absent from Shaw S4 (Smith-Maxwell et al., 1998b).

From studying the voltage dependence of charge movement of ILT, we know that gating currents begin to activate at −130 mV and that charge movement between closed states saturates around −40 mV. Therefore, a prepulse to −140 mV should draw ILT channels into the closed state furthest from the open state, which will maximize the amount of delay in activation.

The behavior of the ILT gating currents suggests that a prepulse to 0 mV should pool ILT channels into the final closed state adjacent to the open state, which will minimize the amount of delay in the time course of activation.

The results of prepulse experiments on the time course of activation of Shaw S4 and ILT are presented in Fig. 8. The time course of Shaw S4 ionic currents is insensitive to the choice of prepulse voltage for all voltages tested (−180 to 0 mV). This result confirms that there are no slow charge-moving transitions between closed states that may have escaped detection in our gating current measurements.

In contrast, the ILT current traces clearly show that prepulses to −140 mV induce a small amount of delay and prepulses to 0 mV relieve this delay. When patches containing ILT channels are prepulsed to 0 mV, which effectively removes the closed state transitions from the ILT activation pathway, the time course of activation of ILT is more like that of Shaw S4 at all voltages (see superimposed Shaw S4 and ILT current traces of Fig. 8 A, bottom). Thus, the small increase in the amount of de-

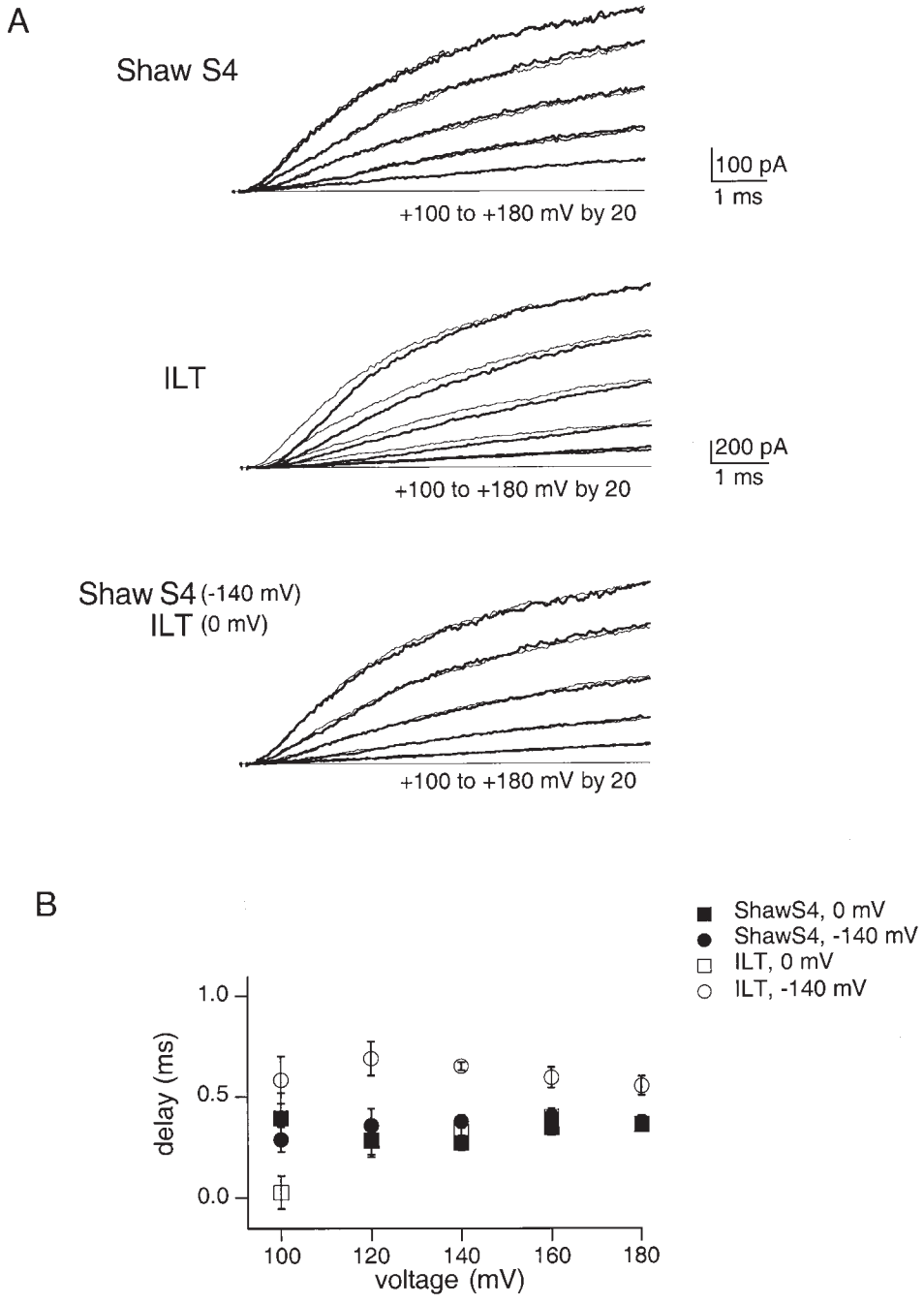

FIGURE 8. Effects of prepulse voltage on the time course of activation of Shaw S4 and ILT. (A) Macroscopic ionic currents of Shaw S4 and ILT recorded after 100-ms prepulses to either 0 mV (thin lines) or −140 mV (thick lines) from a holding voltage of −80 mV. At the bottom of A, ionic currents of ILT recorded after a 0-mV prepulse and Shaw S4 recorded after a −140-mV prepulse are shown superimposed; to enable comparison across patches with different amounts of ionic current, current traces were scaled to superimpose. Currents were elicited by positive voltage steps to the voltages indicated. (B) The amount of delay at the beginning of the time course of activation for different prepulse voltages plotted over a range of test-pulse voltages. The voltage of the prepulse is indicated beside the name of the channel in the symbol legend. Error bars represent the SEM. Mean values were calculated from seven patches each for Shaw S4 and ILT. The amount of delay was determined from the x intercept of single exponential fits to current traces as outlined in MATERIALS AND METHODS.

lay in the ionic currents of ILT at voltages above +140 mV observed by Smith-Maxwell et al. (1998b) can be accounted for by the presence of transitions between closed states in the activation pathway.

The amount of delay present in traces was quantitated by taking the x intercept of single exponential fits to current traces (Fig. 8 B). The amount of delay measured is very small, even for ILT after prepulses to −140 mV. However, a simple first-order reaction (e.g., between a closed state and the open state) would produce a time course of activation with no delay. The small amount of delay observed in Shaw S4 traces that remains in ILT traces after prepulses to 0 mV is consistent with either a highly cooperative transition or with the presence of multiple charge-moving transitions. Since our gating current data indicate that there is only one charge-moving transition in this voltage range for Shaw S4 and ILT activation, the former explanation seems more likely. The small amount of delay observed for Shaw S4 and ILT after prepulses to 0 mV and the small rising phase on the gating currents are both consistent with a cooperative conformational change in which the movement of each subunit facilitates the others.

Mutations at Charged Residues Affect Charge Movement between Closed States

The voltage dependence of the cooperative opening transition is the same for ILT and Shaw S4, but there is no detectable charge movement between closed states in the activation pathway of Shaw S4 in the voltage range of −240 to 0 mV, where a large component of the ILT gating charge moves. The S4 sequence of Shaw S4 has charge-changing substitutions at three positions occupied by basic residues (R1, R2, and K7) in *Shaker* and ILT, resulting in a decrease in the net charge of the S4 from +7 to +3. To test if increasing the net S4 charge of Shaw S4 could rescue the charge movement between closed states, we constructed a mutant, Shaw S4:RRK, that contains all seven of the basic residues present in *Shaker* and all eight of the substitutions at noncharged residues present in the Shaw S4 chimera (see Fig. 1).

The properties of the ionic currents of Shaw S4:RRK are summarized in Fig. 9. The voltage range of activation of Shaw S4:RRK is shifted negatively relative to ILT, but the slope of the conductance–voltage relation of Shaw S4:RRK is similar to that of ILT and considerably more shallow than that of *Shaker*. The time course of activation of Shaw S4:RRK shows little delay and is well described by a single-exponential function over the activation voltage range, consistent with the pres-

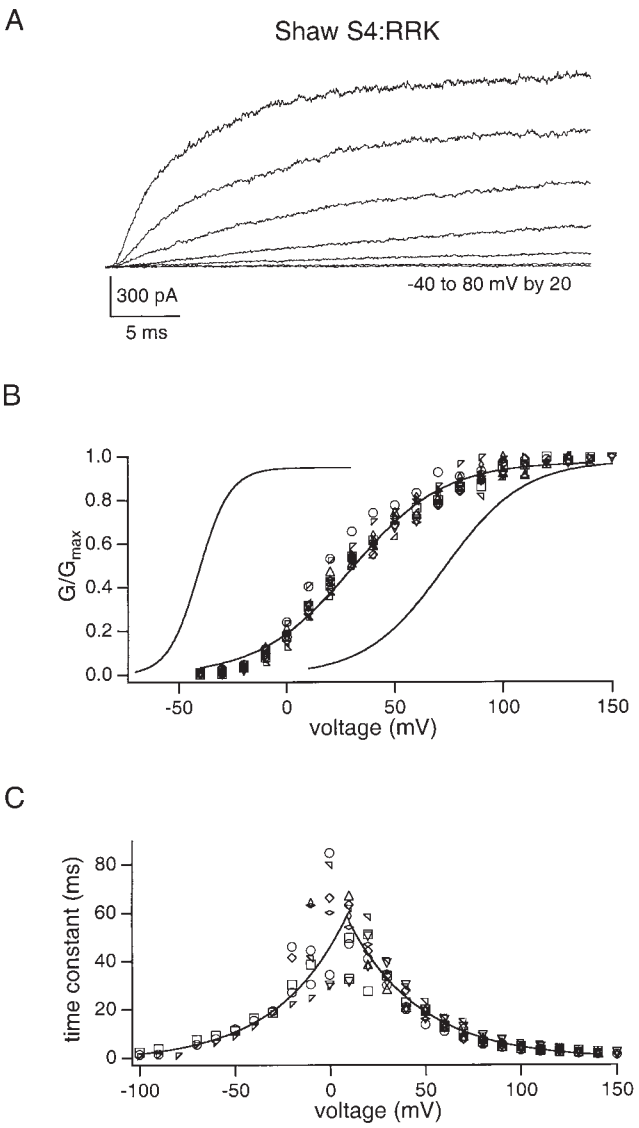

ited by steps to −40 to +80 mV in 20-mV increments, from a prepulse of −100 mV. (B) Normalized conductance as a function of voltage. Shaw S4:RRK data from 11 patches are shown in open symbols; each symbol represents a different patch. The smooth curves represent fits of a Boltzmann function to mean values of normalized conductance for Shaw S4:RRK, *Shaker* (left), and ILT (right). Fits to *Shaker* and ILT are included to facilitate direct visual comparison of the properties of the *GV* for the different channels. Normalized conductance–voltage curves were constructed as described in MATERIALS AND METHODS. The values from these fits are as follows, with *n* representing the number of experiments used to calculate each mean: *Shaker*: $V_{1/2}$ = −40.6 mV, slope factor = 7.2 mV, *n* = 8; Shaw S4:RRK: $V_{1/2}$ = +29.9 mV, slope factor = 21.2 mV, *n* = 6; ILT: $V_{1/2}$ = +72.9 mV, slope factor = 18.3 mV, *n* = 6. (C) Time constants of activation and deactivation of Shaw S4:RRK (open symbols) as a function of voltage. Time constants were obtained from fits of single exponential functions to current traces during activation and deactivation, as described in MATERIALS AND METHODS. Shaw S4:RRK time constants were measured from nine patches. Single exponential fits (smooth curves) to the voltage dependence of the mean activation data (+10 to +140 mV) and the mean deactivation data (−100 to +10 mV) show equivalent charge values of 0.95 and 0.94 e_0, respectively.

FIGURE 9. Properties of macroscopic ionic currents of Shaw S4:RRK. (A) Representative ionic current traces of Shaw S4:RRK elic-

ence of a rate-limiting step in the activation pathway. The time constants of activation and deactivation of Shaw S4:RRK are similar to those of ILT in their amplitude and voltage dependence (Fig. 9 C), but the relationship has been shifted to a more negative voltage range. Analysis of the voltage dependence of channel kinetics indicates that, for the Shaw S4:RRK mutant, 0.94 e_0 are associated with channel opening and 0.95 e_0 with channel closing, for a total of 1.89 e_0 associated with the rate-limiting cooperative transition. These equivalent charge values for the forward and backward rates of the rate-limiting transition are very similar to the charge estimates obtained for ILT of (0.84 e_0 for channel opening and 0.90 e_0 for channel closing, for a total of 1.74 e_0) and for Shaw S4 (0.78 e_0 for channel opening and 0.86 e_0 for channel closing, for a total of 1.64 e_0) (Smith-Maxwell et al., 1998b).

Overall, the properties of the ionic currents of Shaw S4:RRK are very similar to those of ILT and Shaw S4, suggesting that the properties of the rate-limiting final cooperative step in the gating pathway have not been changed by the substitutions at R1, R2, and K7, except for a shift in its voltage-dependent equilibrium. The ionic current properties of Shaw S4:RRK might be expected to resemble those of ILT and Shaw S4 because the Shaw S4:RRK mutant includes all of the substitutions (i.e., the ILT mutations V369I, I372L, and S376T) necessary to make the last cooperative gating transition rate limiting (Smith-Maxwell et al., 1998b).

To investigate the effects of the Shaw S4:RRK mutation on earlier transitions in the activation pathway, we examined the properties of the gating currents (Fig. 10). We found that Shaw S4:RRK gating currents can be recorded at voltages that are more negative than the voltage range of channel opening, demonstrating the presence of charge-moving conformational changes between closed states in the activation pathway. However, the gating currents of Shaw S4:RRK are quite different from those of *Shaker* and ILT (Fig. 10). The midpoint of the charge–voltage curve of Shaw S4:RRK is shifted to an even more negative voltage range and its slope is even more shallow than that of ILT (Fig. 10 B). Moreover, the behavior of the ON gating currents is not consistent with a simple voltage shift relative to *Shaker* and ILT. The time constants of Shaw S4:RRK are considerably slower and have a noticeably more shallow voltage dependence than the time constants for *Shaker* and ILT gating currents (Fig. 10 C; also, note the difference in time scale used to display the Shaw S4:RRK gating currents in Fig.10 compared with *Shaker* and ILT in Fig. 4).

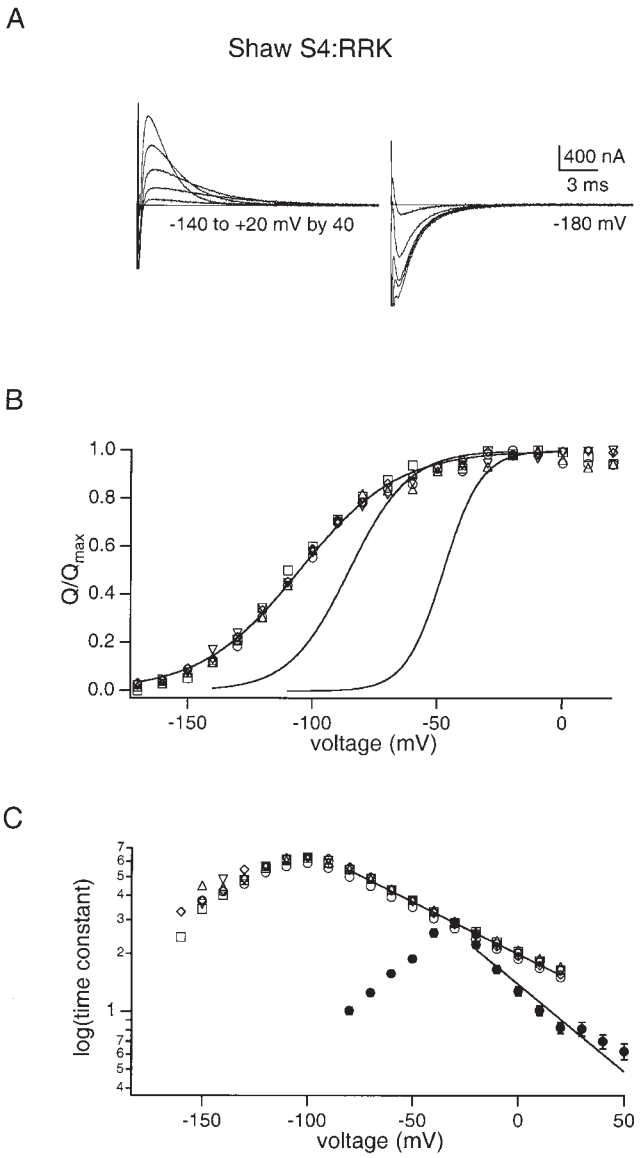

FIGURE 10. Gating currents of Shaw S4:RRK. (A) Representative gating current traces from cut-open oocyte clamp recordings of nonconducting Shaw S4:RRK. ON gating currents were elicited by steps to −140 to +20 mV in 40-mV increments from a prepulse potential of −180 mV. OFF gating currents were elicited by returning the membrane potential to −180 mV after the test pulse. The first 20 ms of the ON and OFF gating current traces are shown. (B) Voltage dependence of charge movement of Shaw S4:RRK (open symbols). The smooth curves represent fits of a Boltzmann function to mean charge data of Shaw S4:RRK, *Shaker* (far right), and ILT (middle). The values for the fits are as follows, with n representing the number of experiments used to calculate each mean: Shaw S4:RRK: $V_{1/2}$ = −106.9 mV, slope factor = 18.3 mV, n = 5; *Shaker*: $V_{1/2}$ = −48.24 mV, slope factor = 7.1 mV, n = 6; and ILT: $V_{1/2}$ = −86.11 mV, slope factor = 11.3 mV, n = 4. (C) Semi-logarithmic plot of time constants of decay of ON gating currents of Shaw S4:RRK (open symbols) and *Shaker* (filled circles) as a function of voltage. For Shaw S4:RRK, each symbol represents one of five different experiments. For *Shaker*, the symbols represent mean values calculated from seven experiments; error bars represent SEM. Time constants were determined by fitting the declining phase of the ON gating currents with single exponential functions. Smooth lines represent fits of the time constant data to single exponential functions with equivalent charge values of 0.58 e_0 for *Shaker* and 0.31 e_0 for Shaw S4:RRK.

The Shaw S4:RRK OFF gating currents are also much slower than those of *Shaker* and ILT.

The relationship between gating charge movement and activation of ionic currents of Shaw S4:RRK is summarized in Fig. 11. (Fig. 11, top) The charge- and conductance-voltage curves are plotted on the same graph. The threshold at which ionic currents can be detected is −30 mV. The charge–voltage curve has reached apparent saturation by –30 mV and does not increase with increasingly positive voltage steps in the voltage range considered (up to +20 mV), despite the fact that an additional component of charge movement would be expected to move during the rate-limiting transition to channel opening in this voltage range. However, the charge movement associated with the rate-limiting transition is too slow to be detected in the ON gating currents in the voltage range of −30 to +20 mV. We did not attempt to measure gating currents at still higher voltages, where the charge moved during the rate-limiting transition would be fast enough to measure, because outward currents develop at higher voltages in the cut-open oocyte configuration and interfere with measurements of gating currents.

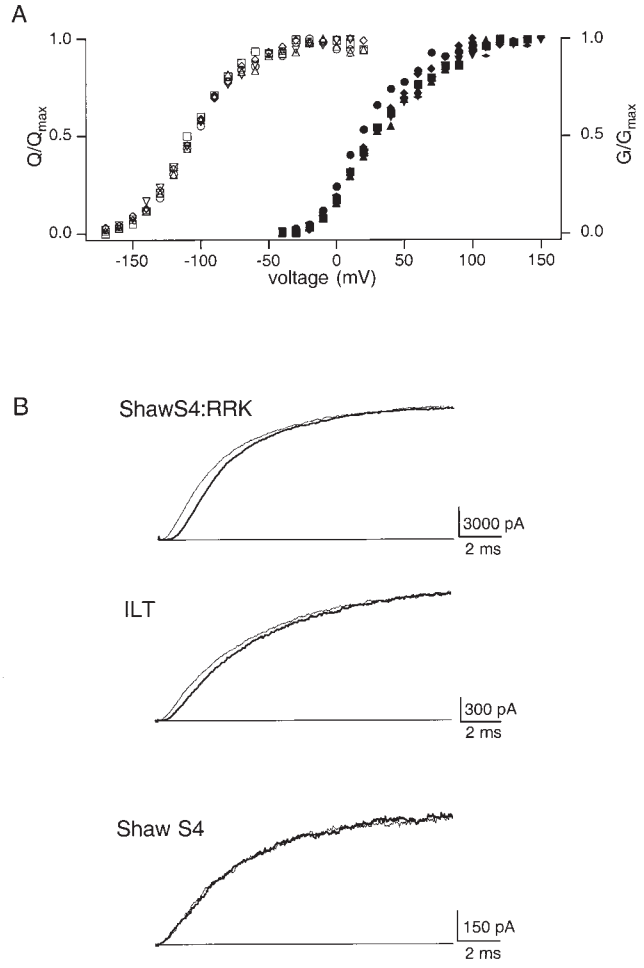

FIGURE 11. Relationship between charge movement and activation in Shaw S4:RRK. (A) Voltage dependence of ON gating charge (left axis, open symbols) and normalized conductance (right axis, filled symbols) of Shaw S4:RRK. The threshold at which ionic current can be detected is −30 mV. (B) Effect of prepulse voltage on time course of activation for Shaw S4, ILT, and Shaw S4:RRK. For Shaw S4:RRK, currents were elicited by steps to +100 mV after a prepulse to −40 (thin lines) or −140 (thick lines) mV. For ILT and Shaw S4, currents were elicited by steps to +160 mV after prepulses to 0 (thin lines) or −140 (thick lines) mV. Similar results were seen in five patches of Shaw S4:RRK, seven patches of ILT, and seven patches of Shaw S4.

To test whether or not these closed states are coupled to channel opening, we can look for an increase in the amount of delay in the time course of activation with appropriately negative prepulses. The traces shown in Fig. 11 B demonstrate that the amount of delay in the time course of activation of Shaw S4:RRK can be increased by a prepulse to −140 mV and decreased by a prepulse to −40 mV. Therefore, the voltage-dependent transitions between closed states that we detected as gating currents are traversed in the activation pathway. For comparison, current traces are also shown from similar experiments performed on ILT and Shaw S4. The relatively large delays in the ionic currents of Shaw S4:RRK produced by negative prepulse voltages are consistent with the slow kinetics of its gating currents compared with those of ILT.

The relationship between the gating behavior of Shaw S4:RRK, ILT, and Shaw S4 is consistent with the idea that the rate-limiting transition is late in the activation pathway and with previous work that has shown that R1 and R2 move through the membrane electric field during early gating transitions and that K7 never crosses the electric field (Larsson et al., 1996; Baker et al., 1998). The rate-limiting transition in the Shaw S4:RRK activation pathway displays a voltage dependence similar to that of ILT and Shaw S4, suggesting that the charges at R1, R2, and K7 do not traverse the membrane electric field during the final cooperative transition. The gating current recordings and Cole-Moore type experiments on ILT, Shaw S4, and Shaw S4:RRK confirm that R1, R2, and K7 traverse the membrane electric field during earlier gating transitions.

A Kinetic Model for ILT

To further understand the changes introduced by the ILT mutation, we modified a kinetic model that was developed for *Shaker*. The rationale for modifying a *Shaker* model is that the ILT mutation should not grossly alter the gating mechanism because the amino acid substitutions introduced into the protein by this mutation are very conservative, producing small changes in the size and shape but not the chemistry of the amino acid side chains. In support of this idea, the gating currents of ILT in the −140- to 0-mV range were found to resemble those of *Shaker*, indicating that ILT and *Shaker* un-

dergo similar numbers and types of conformational changes between closed states. Also, the individual substitution of any one of the amino acids in the ILT mutant (V369I, I372L, S376T) causes much smaller changes in gating than is observed for the ILT triple mutant, suggesting that the structure of the protein readily accommodates each of the individual substitutions (Smith-Maxwell et al., 1998b). The state diagram for the *Shaker* model is shown in Fig. 12 A, and the rates and voltage dependences for the rate constants used are given in Table II.

In this paper, we have used a 16-state model for *Shaker* activation. In this model, each subunit undergoes two sequential independent transitions to reach a final closed state from which the channel opens cooperatively. A single transition has been used to represent the final cooperative transition, which may be more complex. Quantitative agreement between model predictions and *Shaker* data can be improved by addition of more states to this class of kinetic model (see Schoppa and Sigworth, 1998c). In the model of Schoppa and Sigworth (1998c), each subunit undergoes an additional independent transition, followed by two sequential cooperative transitions to reach the open state. However, we have used a 16-state model for *Shaker* because it is the simplest model that adequately describes most of the features of *Shaker* gating and ionic currents.

The 16-state model is similar to the 15-state model proposed by Zagotta et al. (1994b) and Smith-Maxwell et al. (1998b), except in its treatment of the last transition between the final closed state and the open state. In the 15-state model, there is no final closed state from which the channel opens cooperatively. Rather, cooperativity is implemented by slowing the first closing transition. The 15- and 16-state models describe wild-type *Shaker* ionic and gating currents equally well. Both the 15- and 16-state models can be readily adapted to describe the ionic currents of ILT; however, only the 16-state model can be adapted to describe the behavior of ILT gating currents. The 15-state model cannot produce the two well-separated components of gating current that were observed for ILT. This result strongly suggests that the molecular mechanism of cooperativity in the rate-limiting step in the activation of ILT is a highly cooperative step rather than a stabilization of the open state. The ability of a 16-state model to describe simultaneously the gating and ionic currents of ILT suggests that a 16-state model, in which the channel reaches a final closed state from which it opens cooperatively, represents a more reasonable approximation of the conformational changes of the protein than the 15-state model.

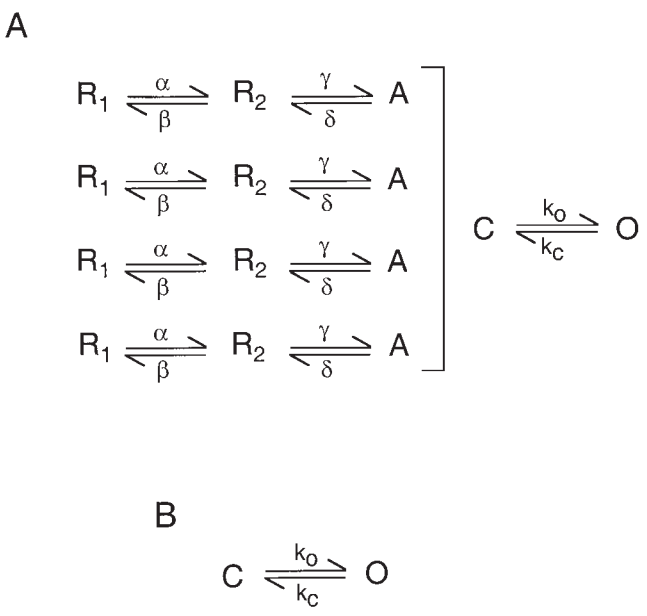

FIGURE 12. (A) Kinetic model for *Shaker* and ILT. This kinetic model is similar to a *Shaker* model developed by Zagotta et al. (1994b) except that the last transition to opening has been treated as a separate step. See text for details. (B) A two-state kinetic model for Shaw S4. The 0-mV rate constants and the associated equivalent charge for all rate constants are given in Table II.

TABLE II

Rate Constants for Models for Shaker, ILT, and Shaw S4

	Shaker		ILT		Shaw S4	
Rate constant	k_0	z_k	k_0	z_k	k_0	z_k
	s^{-1}	e_0	s^{-1}	e_0	s^{-1}	e_0
α	1120	0.2	1120	0.2	—	—
β	373	1.6	15	1.5	—	—
γ	2800	0.3	2800	0.3	—	—
δ	21.2	1.1	6	1.0	—	—
k_0	3000	0.1	1	1.0	1	1.0
k_c	250	0.3	70	0.8	70	0.8

Rate constants are given for the models presented in Fig. 9. The k_0 column gives the 0 mV rate for each rate constant and the z_k column indicates the equivalent electronic charge assigned to the rate constant. Rate constants were assumed to be exponentially dependent on voltage. For example: $k = k_0 e^{(zFV/RT)}$, where k_0 is the 0 mV rate in s^{-1}, z is the equivalent electronic charge in e_0, F is the Faraday constant, V is voltage, R is the universal gas constant, and T is temperature in Kelvin.

The model predictions for wild-type *Shaker* and ILT gating currents are compared with data in Fig. 13. The wild-type *Shaker* model does a good job of predicting many features of the *Shaker* gating currents, including a rising phase in the ON gating currents, a rising phase in the OFF gating currents associated with channel opening, and the position and steepness of the steady state voltage dependence of gating charge movement. The predictions for the time constants of decay of the ON gating currents agree well with the data over the −30- to +50-mV range, but less well in the −70- to −40-mV range, as was also observed in the 15-state model of Zagotta et al. (1994b). The agreement between the pre-

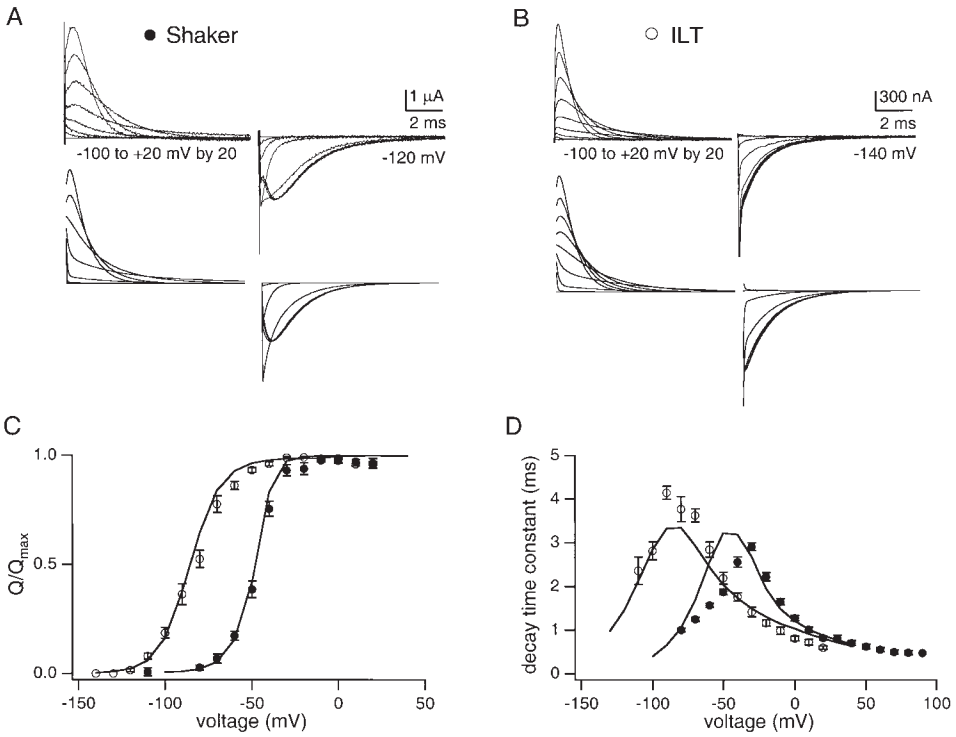

FIGURE 13. Comparison of observed *Shaker* and ILT gating currents to model predictions. (A) Comparison of *Shaker* gating current traces from cut-open oocyte clamp recordings (top) to those predicted by the *Shaker* model (bottom). ON gating currents were elicited by steps to −100 to +20 mV in 20-mV increments from a prepulse to −120 mV. OFF gating currents were elicited by steps down to −120 mV after the test pulse. For a complete description of the voltage protocols, refer to MATERIALS AND METHODS. (B) Comparison of ILT gating current traces from an inside-out patch recording (top) to those predicted in the ILT model (bottom). ON gating currents were elicited with steps to −140 to +20 mV in 20-mV increments from a prepulse to −140 mV. OFF gating currents were elicited by steps down to −140 mV after the test pulse. (C) Voltage dependence of charge movement and (D) voltage dependence of time constants of the decay of the ON gating currents for *Shaker* (●), ILT (○), with the *Shaker* and the ILT model predictions shown as solid lines superimposed on the data. Normalized charge–voltage curves were constructed from the ON gating currents as described in MATERIALS AND METHODS. Time constants were obtained by fitting the declining phase of the ON gating currents with single exponential functions. The data were obtained from six experiments for *Shaker* and six experiments for ILT. Error bars represent SEM.

dictions of the time constant of decay of the ON gating currents is improved significantly by adding a third independent transition per subunit (Schoppa and Sigworth, 1998c).

The gating current predictions for the ILT model are presented in two parts. In Fig. 13, the model predictions for gating currents in the −140- to +20-mV range, where charge moves between closed states, are compared with ILT data in the same voltage range. In Fig. 14, the model predictions for gating currents in the voltage range of channel opening are compared with ILT data.

To reproduce the behavior of ILT gating currents in the −140- to 0-mV range, it was necessary to slow both of the independent backward transitions in each subunit relative to wild type *Shaker*, without changing the independent forward transitions. The largest change to the model was a 25-fold slowing of the rate of the β transitions. The rate of the δ transitions was slowed to a lesser degree, 3.5-fold. The fit of the model to the data was improved somewhat by slightly decreasing the amount of charge assigned to the independent backward transitions. These alterations to the backward transitions are sufficient to reproduce the features of the ILT gating currents at negative voltages, including the shift in the voltage dependence of the time constants and charge movement, the decrease in the slope of the charge movement, and the overall time course of the ON and OFF gating currents. Because the forward transitions are unchanged, the time constants of decay of the ON gating currents converge with those of the *Shaker* model at 0 mV (Fig. 13 D), as can be observed in the data (see Fig. 4 D). Although the voltage dependence of the last concerted transition must be increased for the ILT model, the total amount of gating charge assigned is very similar to that of the model for wild-type *Shaker*: 13.8 e_0 for ILT and 13.2 e_0 for *Shaker*.

To reproduce the gating currents of ILT in the voltage range of channel opening, the forward and backward rates of the final cooperative transition in the 16-state *Shaker* model must both be slowed and their voltage dependences must be increased relative to wild-type *Shaker*. The forward and backward cooperative transitions have been assigned equivalent charge values of 1.0 and 0.8 e_0, respectively, for a total of 1.8 e_0 assigned to the final cooperative transition. The parameters used in this paper for the forward and backward transitions of the final cooperative step are the same as in the model for ILT gating proposed by Smith-Maxwell et al. (1998b). The ionic currents predicted by the ILT model proposed in this paper are indistinguishable from those predicted by the model of Smith-Maxwell et

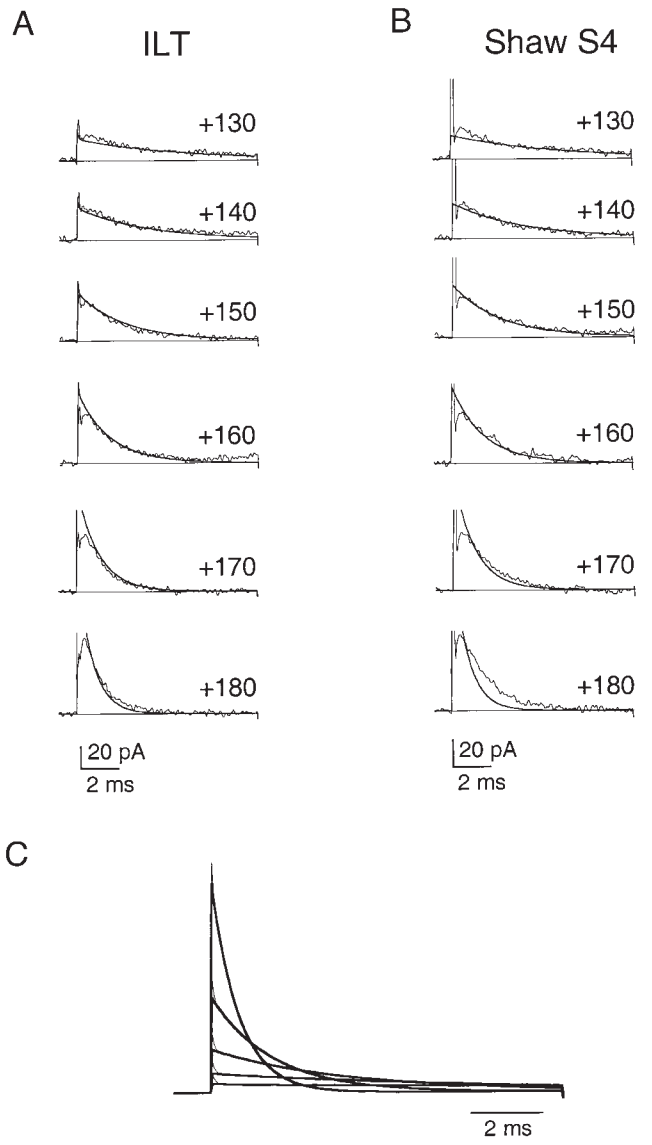

FIGURE 14. Comparison of ILT and Shaw S4 ON gating currents in the voltage range of channel opening to those predicted by the 16-state ILT model and the 2-state Shaw S4 model, respectively. (A) ILT ON gating currents in the voltage range of channel opening are shown with traces predicted by the 16-state model (smooth lines) superimposed. For both ILT and the model simulation, ON gating currents were elicited by 10-ms steps to the voltages indicated from a holding voltage of 0 mV. The model traces were scaled to reflect the number of channels in the patch by normalizing to the current level at 1 ms in the +160-mV traces. (B) Shaw S4 ON gating currents in the voltage range of channel opening are shown with traces predicted by the 2-state model (smooth lines) superimposed. For both Shaw S4 and the model simulation, ON gating currents were elicited by 10-ms steps to the voltages indicated from a holding voltage of 0 mV. The model traces were scaled as described in A. The currents in A and B were filtered at 9 kHz during recording, but for this figure, the traces were digitally filtered at 4 kHz to reduce noise and facilitate comparison of data to model-predicted waveforms. (C) Comparison of the ON gating currents in the voltage range of channel opening predicted by the 16-state ILT model (thin lines) and the 2-state Shaw S4 model (thick lines). The current traces were scaled as described in (A). The currents predicted by the two different models are essentially indistinguishable after the first 200 μs.

al. (1998b) (data not shown), despite the fact that the kinetic model was modified in this paper to incorporate ILT gating current data between −140 and 0 mV. In this model, the voltage dependence of the last cooperative step must be increased significantly to reproduce ILT behavior, from 0.4 e_0 for wild-type *Shaker* to 1.8 e_0 for ILT. However, the true voltage dependence of the last cooperative transition in wild-type *Shaker* is not known for certain because the transition is too fast to be investigated thoroughly. The nature of the last cooperative step in wild-type *Shaker* will be discussed further in DISCUSSION.

Gating current simulations were elicited from a holding voltage of 0 mV to isolate the component of charge that moves in the activation range. The model predictions are shown superimposed on representative ILT current traces in Fig. 14 A. The model does a very good job of predicting the overall time course of ILT gating charge movement over a wide voltage range, +130 to +180 mV. The ILT model predictions were compared with ILT gating currents from four different patches, and the agreement between the model and the gating currents was very good for all four patches over the range of +130 to +180 mV.

However, the model does not predict the small rising phase that is observed in the gating current recordings. This discrepancy probably occurs because we have used a concerted step (e.g., a single transition in which all of the channel subunits move in unison) as an approximation for the cooperative step. A concerted step can be thought of as an extreme case of cooperativity. The presence of a small rising phase in the time course of the ILT gating currents at high voltages suggests that the channel undergoes a conformational change that is highly cooperative but not concerted.

Overall, the gating currents in the voltage range of channel opening of ILT are well described by the model over a wide voltage range. The fit of the model to the data provides additional evidence that the rate-limiting cooperative transition in the gating of ILT is the final transition in the gating pathway.

A Kinetic Model for Shaw S4

We used a two-state model for Shaw S4 because it is consistent with the single-exponential time course of the ionic currents and the absence of gating currents at voltages outside the activation voltage range. The state diagram for the model is shown in Fig. 12, and the rates and voltage dependence for the rate constants used are given in Table II. The values used for the rates in the

two-state model are the same as those used for the final transition in the ILT model.

For the purpose of comparison, the gating current predictions of the two-state Shaw S4 model and of the multi-state ILT model in the voltage range of channel opening have been presented together in Fig. 14. All gating current simulations were elicited from a holding voltage of 0 mV. The gating current predictions from the ILT and Shaw S4 models are indistinguishable, except during the first 200 μs after depolarization (traces are shown superimposed in Fig. 14 C). It is unlikely that we would detect this difference in our recordings, since the first 200 μs after a step to a new voltage is typically obscured by capacitive transients.

The Shaw S4 model predictions were compared with Shaw S4 gating currents from four different patches. The model predictions agree very well with the Shaw S4 gating current recordings over the voltage range of +130 to +160 mV, but around +170 mV the predictions of the model and the recorded currents start to diverge. The model predictions are apparently too fast at the highest voltages. We observed a similar but smaller divergence between model and data for ILT at +180 mV and higher. The degree to which model and data diverged was consistently greater for Shaw S4 than ILT but varied from patch-to-patch for both channels.

The divergence between model and data may indicate that the true channel behavior is more complicated than presented in the model. For example, our model does not include any transitions of the open channel to closed states that are not in the activation pathway. Open *Shaker* channels can close to closed states that are outside of the activation path, and the rates for some of these transitions exhibit a small voltage dependence (Hoshi et al., 1994; Schoppa and Sigworth, 1998a). These transitions may make an increasingly significant contribution to the voltage-dependent and kinetic behavior of the channel as the open probability approaches its maximum. Further, the rates of transitions to closed states outside of the activation path can be affected by mutations (Schoppa and Sigworth, 1998b). The difference between the gating currents of ILT and Shaw S4 at high voltages might indicate that Shaw S4 and ILT have different effects on the transitions from the open state of the channel to states outside of the activation pathway.

DISCUSSION

The simplest interpretation of the gating phenotype of the ILT mutant is that the ILT mutation has uncovered the final voltage-dependent cooperative transition in the *Shaker* activation pathway by making it rate limiting. The most compelling evidence for this interpretation is the close agreement between the amount of gating charge moved in the voltage range of channel opening and the amount of charge moved in the forward and backward transitions of the rate-limiting step, as estimated from fits to time constants of activation and deactivation. This result strongly suggests that the rate-limiting cooperative transition is the only charge-moving transition in the voltage range of channel opening, and therefore it must be the last transition in the activation pathway. This interpretation of our results is further supported by the fact that the voltage dependence of the ILT gating current kinetics at high voltages is the same as the voltage dependence of the ionic currents.

However, the kinetics of the ILT gating currents are noticeably faster than the ionic currents, when they should be the same if the gating charge movement is associated with the rate-limiting cooperative transition. It is important for our interpretation of the gating current data to consider the nature of this discrepancy and plausible mechanisms by which it could be produced.

Since the ionic and gating current kinetics have the same voltage dependence, the difference in their kinetics can be interpreted as a voltage shift of ~20 mV. If a single charge-moving transition determines the properties of the conductance–voltage and charge–voltage curves, then a 20-mV voltage shift can be produced by a rather small energetic difference of ~0.8 kcal mol^{-1}, using the relationship:

$$\Delta\Delta G = z\Delta V_{1/2},$$

where z is the amount of charge moved for the final transition and $\Delta V_{1/2}$ is the difference in the voltage of half-maximal activation between the gating and ionic currents. An energetic difference of ~0.8 kcal mol^{-1}, and hence a 20-mV voltage shift in the gating currents, could be produced by a number of different mechanisms. We will discuss two mechanisms for which there is experimental evidence, namely, the effects on gating of the nonconducting conditions (the W434F mutation) used to measure gating currents, and variability in voltage-dependent behavior between patches.

To record gating currents without interference from ionic currents, we rendered channels nonconducting by introducing the W434F mutation into the pore region (Perozo et al., 1993). Originally, the W434F mutation was thought to block conduction of ions through the pore of the open state of the channel without interfering with activation gating transitions (Perozo et al., 1993). However, several lines of evidence now indicate that the W434F mutation does not simply block conduction of ions and does affect gating near the open state of the channel. It has been shown that the W434F mutation decreases the probability of being open to $\sim 10^{-5}$ by inactivating the channel, but does not block conduction in a normal open state conformation (Yang et al., 1997). Further, Chen et al. (1997) found that the

W434F mutation at the homologous position in Kv1.5 slows the return of OFF gating currents after steps to voltages where the channel opens (Chen et al., 1997). These results clearly demonstrate that the W434F mutation alters transitions near the open state of the channel, either between the last closed state in the activation pathway and the open state or between the open state and closed states that are not traversed in the activation pathway.

To date, there is no direct evidence demonstrating that the kinetics of the activation pathway are affected by the W434F mutation. However, charge movement associated with slower gating transitions could mask effects of the W434F mutation on very fast transitions. Wild-type *Shaker* undergoes a very fast forward transition (time constant of $\sim$100 μs) near the open state (Schoppa and Sigworth, 1998a). Changes in the kinetics of this transition would be difficult to resolve even if they were relatively large because the transition is an order of magnitude faster than the charge movement measured in our gating current records. If the W434F mutation changes the energy of the final gating transition by as little as $\sim$0.8 kcal mol^{-1} (e.g., the energy difference that is observed between the ON gating current of ILT and the ionic currents), it would not cause a measurable change in the ON gating currents of *Shaker*. However, the ILT mutation may unmask the effects of the W434F mutation on the kinetics of ON gating currents by isolating the last gating transition.

The observed voltage shift may also be due, at least in part, to variability between patches. Variability in voltage-dependent behavior between patches has been observed in both wild-type and mutant *Shaker* channels (Zagotta et al., 1994b; Schoppa and Sigworth, 1998b,c). The cause of this variability is not known, but it may be the result of the action of various factors (e.g., kinases, phosphatases, redox agents) that are present in oocytes. Our ILT and Shaw S4 gating current experiments may be unusually biased in this respect because of the extraordinary levels of channel expression that were required to produce a measurable signal for the small component of gating current at high voltages. As a result, all of these recordings were obtained from two batches of oocytes with exceptionally high levels of expression, and the gating current recordings will be biased towards the conditions found in these particular batches of oocytes. Further, because of the need for higher protein expression levels, gating currents were typically recorded from much older oocytes than those used to record ionic currents, and the age of the oocytes may be a factor in modification of channel by such agents as phosphatases and kinases. Meanwhile, ILT and Shaw S4 ionic currents could be measured from many batches of oocytes and, interestingly, the variability observed between patches has been considerable: the standard deviation of the midpoint of the conductance–voltage curve is ±10 mV (Smith-Maxwell et al., 1998b). Such large variability in the midpoint of the conductance–voltage curve exceeds that expected based on series resistance errors, as error due to series resistance in our experiments was generally <2 mV.

We cannot rule out the possibility that the voltage shift (energy difference) observed between the kinetics of our ILT gating and the ionic currents is real and that the gating mechanism of ILT is actually more complicated than the mechanism presented in this paper. However, it is reasonable to suggest that the underlying small energy difference could be introduced by either the W434F mutation or the different experimental conditions required to obtain gating currents versus ionic currents. If the voltage shift is corrected for, the amplitude and voltage dependence of the kinetics of the gating currents recorded in the voltage range of channel opening are consistent with those expected to accompany the gating charge movement during the last cooperative transition that opens the channel. Therefore, in spite of the voltage shift, it seems likely that the charge movement that we have measured corresponds to the charge moved in the rate-limiting cooperative step.

Insights into the Activation Pathway

The ability to study the gating process in wild-type *Shaker* is limited by the fact that it is difficult to study individual transitions independently of one another because the rates and voltage dependences of most of the transitions in *Shaker* activation are too similar (Zagotta et al., 1994b). The ability to perturb the energies of gating transitions with mutations provides a means to dissect out steps in the gating pathway. For this reason, we have studied the effects of mutations in the S4 region in detail and interpreted the effects of the mutations, when possible, in the context of a kinetic model for *Shaker*. Using a similar approach, Schoppa and Sigworth (1998b,c) have gained insights into the gating mechanism of *Shaker* using the V2 mutant.

For most of this discussion, we will focus on the ILT mutation, since it does not introduce any charge-changing substitutions into the S4 of *Shaker* and has been shown to be the least disruptive to the overall gating pathway of the three mutants in this study. Because the ILT mutation makes the last cooperative gating transition in activation rate limiting, we can study the properties of this transition in isolation from other gating transitions. Through analysis of the voltage dependence of ionic and gating currents, we have been able to determine that the equivalent charge associated with this transition is $\sim$1.8 e_0, and we have shown that the rate-limiting cooperative transition is the final voltage-dependent transition in the gating pathway of ILT.

Our results also provide insight into the manner in which cooperativity is implemented in the activation pathway. Activation of wild-type *Shaker* can be described adequately with models in which cooperativity is implemented in one of two ways: (a) as a cooperative stabilization of the open state, as in the 15-state model of Zagotta et al. (1994b), or (b) as a final cooperative transition(s) to the open state (this paper; Schoppa et al., 1992; Schoppa and Sigworth, 1998c). However, our analysis of the ILT gating currents clearly supports the existence of a final cooperative transition in the activation pathway.

Two lines of experimental evidence suggest that there is a similar but much faster cooperative transition to the open state in the activation pathway of wild-type *Shaker*. Zagotta et al. (1994b) found that the first closing transition in *Shaker* is slower than earlier backward transitions, consistent with the presence of a strongly forward-biased cooperative transition between the final closed state of the channel and the open state (e.g., a transition with a very fast forward rate and relatively slow backward rate). But they concluded that if there is a forward cooperative transition before channel opening, it is sufficiently fast as to be "silent" in measurements of the activation kinetics of *Shaker*. Recently, Schoppa and Sigworth (1998a) have used reactivation voltage protocols to uncover a strongly forward-biased cooperative transition near the open state. They found that the forward transition is very fast, at least as fast as 9,100 s^{-1} (which corresponds to a time constant on the order of 100 μs). However, their estimate of the rate and voltage dependence of this transition should be considered as a lower bound because the time course of such a fast transition may not be fully resolved from the contribution of other slower transitions to the time course of reactivation. Cooperative interactions in proteins can occur on time scales much faster than 100 μs. For example, haemoglobin undergoes its oxy–deoxyhaemoglobin conformational change in 20 μs (Spiro et al., 1990). Even if such a fast transition could be isolated experimentally from slower transitions in the activation pathway of wild-type *Shaker*, it would be difficult to measure using standard electrophysiological techniques.

The amount of charge assigned to the cooperative final transition in ILT gating, ~1.8 e_0, is greater than the amount of charge assigned to the final opening transition of *Shaker* in all kinetic models of *Shaker* (this paper; Zagotta et al., 1994b; Bezanilla et al., 1994; Schoppa and Sigworth, 1998c), except for an early model presented by Schoppa et al. (1992). There is no consensus between the various models on the voltage dependence of the final opening transition in wild-type *Shaker*, which reflects the fact that it is difficult to measure such a fast transition as a separate component in the kinetic measurements. The ILT mutation makes the final cooperative transition rate limiting, making it possible to measure the voltage dependence of this transition in the ILT mutant.

Is the voltage dependence of the final cooperative transition in wild-type *Shaker* similar to that of ILT? The results of studies on the V2 mutant, which substitutes a valine for L382 at the carboxy-terminal border of the S4, may provide insight into this matter (Schoppa et al., 1992; Schoppa and Sigworth, 1998b,c). The V2 mutation causes a large positive shift in the voltage dependence of a component of gating charge of ~1.8 e_0 and shifts the probability of channel opening to a much more positive voltage range than *Shaker*. In these respects, the effect of the V2 mutation is strikingly similar to that of the ILT mutation. However, in the kinetic model for *Shaker* and V2 gating developed by Schoppa and Sigworth (1998c), the voltage-shifted component of gating charge (1.75 e_0) is moved in not one but two sequential concerted transitions preceeding channel opening, each of which moves ~1 e_0. The primary reason cited for introducing two final cooperative transitions is to explain the features of *Shaker* and V2 OFF gating currents, which show a rising phase followed by a slow decay. Schoppa and Sigworth (1998c) found that one cooperative transition must be introduced to account for the rising phase of the OFF gating currents, and a second cooperative transition must be introduced to account for the slow decay, which is slower than the independent intermediate gating transitions. However, the kinetics of the OFF gating currents, specifically the presence of a rising phase, may be affected by channels opening under nonconducting conditions (Chen et al., 1997). The question of the validity of the rising phase in the OFF gating kinetics of wild-type *Shaker* could be addressed using the experimental approach of Chen et al. (1997), whereby OFF gating currents are measured in conducting solutions by stepping to the reversal potential of the solutions.

It is not clear how to reconcile our ILT results with the model of Schoppa and Sigworth (1998c). Their model is well constrained by measurements of gating currents, ionic currents, and single-channel currents. However, the time course of activation of the V2 channel is fast and sigmoidal like *Shaker* and, accordingly, the final two cooperative transitions for *Shaker* and V2 in the model (Schoppa and Sigworth, 1998c) are very fast. As in the case of wild-type *Shaker*, the last cooperative transition in the gating of V2 may be too fast to be studied independently of other gating transitions. Thus, it seems plausible that the last cooperative transition has a similar voltage dependence (~1.8 e_0) for *Shaker*, ILT, and V2, and that the disagreement between the models arises because of the difficulties inherent in characterizing the last cooperative transition in *Shaker* and V2.

Interestingly, Smith-Maxwell et al. (1998b) found that the I372L substitution, which is one of the three substitutions made in ILT, is responsible for increasing the equivalent charge movement associated with the final opening transition. The I372L substitution also greatly slows the final transition, which allows the properties of the final transition to be determined. Again, it is possible that the final opening transition in *Shaker* has the same voltage dependence as in the I372L and ILT mutants but that the transition is simply too fast to measure in *Shaker*.

Alternatively, the I372L mutation may have altered the amount of equivalent charge moved during the last cooperative gating transition. It is conceivable that charge-conserving mutations could alter the amount of charge moved during a transition by changing the movement of the voltage sensor, thereby increasing the fraction of the electric field through which the charged residues move or increasing the number of charged residues that interact with the electric field during the transition between the final closed state and the open state.

However, we have found that the amount of charge moved in this step is not readily altered by mutations elsewhere in the S4 sequence. The cooperative transition has the same voltage dependence for all three mutant channels studied in this paper, namely ILT, Shaw S4, and Shaw S4:RRK, despite the fact that these three mutants have different S4 sequences and produce different effects on earlier steps in the gating pathway.

Channel Structure and Conformational Changes during Activation

As yet, we do not understand the molecular basis for structural transitions or cooperativity in *Shaker*. But several aspects of the molecular basis for structural transitions and cooperative interactions are well understood for a handful of allosteric proteins that have been crystallized in both active and inactive conformations (for review, see Perutz, 1989). Flexibility of helix packing seems to be essential for the structural transitions of many allosteric proteins. α-Helices can shift relative to each other by up to 1.6 Å and turn by several degrees with only minor adjustments to their side chain packing. When coupled in series, the small shifts of α-helices can be amplified to produce large structural transitions (e.g., for citrates synthase, haemoglobin, and aspartate transcarbamylase).

The final cooperative transition in *Shaker* gating may have a similar design, in which a series of small shifts and turns of many α-helical regions of the protein produce the structural transition that opens or closes the channel. Consistent with this hypothesis, cysteine-modifying experiments have shown that the process of activation changes the exposure of residues to solution in many regions of the protein, including the S4 region (Larsson et al., 1996; Yusaf et al., 1996), the S4–S5 linker region (Holmgren et al., 1996), and the S6 region (Liu et al., 1997). This hypothesis is also consistent with the collective findings of a number of mutagenesis studies. In addition to the ILT and V2 mutations, a number of mutations have been identified in the S4, S4–S5 linker, and S5 that affect cooperativity by increasing the backward rate of the cooperative transition, which manifests itself as an increase in the first closing rate from the open channel in single channel recordings. These mutations include R3Q in the carboxy-terminal half of the S4 helix (Shao and Papazian, 1993), E395C (Holmgren et al., 1996) in the S4-S5 linker region, and F401I in the amino terminal of the S5 helix (Kanevsky and Aldrich, manuscript submitted for publication). In the *Shaker* literature, there are many additional reports of *Shaker* mutations in the S4–S6 regions that produce strong effects on gating that are consistent with changes in cooperativity but for which the reported data are incomplete or inconclusive (for review, see Sigworth, 1994).

Our knowledge of the structure of *Shaker*, albeit limited, is also consistent with this hypothesis. All of the transmembrane regions of *Shaker* are predicted to be α-helical, and experimental evidence is emerging in support of this prediction. In the three-dimensional structure of the bacterial channel, the sequences corresponding to the S5 and S6 regions of *Shaker* are α-helical (Doyle et al., 1998). Also, evidence from cysteine-scanning mutagenesis suggests that at least part of the S4–S5 linker is α-helical (Holmgren et al., 1996).

This physical model of gating, in which a series of small shifts of many α-helices produce a larger structural transition that opens the channel, can explain why even conservative substitutions like ILT and V2 can produce such strong effects on gating: they may be involved in close-packed contacts between helices that shift during gating. It can also explain why mutations in different regions of the protein affect a single conformational change: extensive regions of the protein move during the conformational change that accompanies channel opening.

The ILT mutant, which isolates the last cooperative gating transition from earlier gating transitions, may provide a valuable experimental tool for dissecting out the molecular basis of structural transitions in the activation of *Shaker*. The ILT channel could be used as a background for cysteine-scanning mutagenesis experiments in regions that have been shown to change their exposure during channel opening, like the S4 region (Larsson et al., 1996; Yusaf et al., 1996) or the S6 region (Liu et al., 1997). With this approach, we could correlate the conformational changes of the protein with either the final cooperative step of the gating pathway or the early charge moving steps.

Role of the S4 in Cooperative Interactions between Subunits

The molecular basis for cooperativity between subunits is not understood for *Shaker*, but it is well understood for a number of allosteric proteins that have been crystallized in active and inactive forms (for review, see Perutz, 1989). Subunit contacts are of critical importance for stabilizing the alternative structures of the active and inactive forms of haemoglobin, phopsphofructokinase, and aspartate transcarbamylase. The contacts between subunits strongly stabilize only the alternative quaternary structures of the protein and do not stabilize intermediate forms of the protein (e.g., where some subunits are in a different conformation from the others). Thus, concerted transitions between alternative quaternary structures of the protein are strongly favored energetically. The contacts between subunits in alternative structures are stabilized chiefly by electrostatic interactions and hydrogen bonds between side chains of opposite charge.

The molecular basis of cooperativity in *Shaker* may have a similar design. The results presented in this paper and Smith-Maxwell et al. (1998a,b) clearly demonstrate that the S4 region is involved in cooperative interactions between subunits, not just in voltage sensing. Although the involvement of the S4 in cooperativity may be mediated indirectly, our results point to the intriguing possibility that the S4 helix may form part of the interface between subunits. If the S4 forms part of the interface between subunits, then it is possible that some of the charged residues in the S4 region participate in salt bridges across subunits that stabilize the alternative quaternary structures of the closed and open *Shaker* channel.

The evidence in favor of the charges in the S4 region participating in salt bridges is compelling. Neutralizations at K5 and R6 are "lethal" (prevent proper folding and expression of channels), but can be rescued by making complementary neutralizations at E293Q in the S2 region and D316N in the S3 region, suggesting that the S4 basic residues K5 and R6 participate in electrostatic interactions (salt bridges) with acidic residues in the S3 (Papazian et al., 1995). Tiwari-Woodruff et al. (1997) have shown that a lethal charge reversal mutation at K5 can be rescued by a second charge reversal mutation at E293 and that a lethal charge reversal mutation at E283 in the S2 can be rescued by making a second charge reversal mutation at either R3 or R4.

Although there is strong evidence to suggest that several of the charges in the S4 region participate in salt bridges, the question of whether these bridges form within or across subunits has not been as thoroughly investigated. Studies on heteromultimeric channels suggest that the interaction between K5 and E293 is within, not across, subunits (Tiwari-Woodruff et al., 1997), but this result alone does not preclude the possibility that some of the charges in the S4 region can participate in salt bridges across subunits.

The authors thank Catherine Smith-Maxwell for her contribution to the development of this project and for valuable discussions throughout the project. We thank Ligia Toro for the kind gift of the W434F construct of *Shaker*.

This work was supported by a grant from the National Institutes of Health (NS-23294). R.W. Aldrich is an investigator with the Howard Hughes Medical Institute. J.L. Ledwell was supported by an NSERC 1967 Science and Engineering Scholarship from the Natural Sciences and Engineering Research Council of Canada.

Original version received 14 October 1998 and accepted version received 6 January 1999.

REFERENCES

Aggarwal, S.K., and R. MacKinnon. 1994. Determination of *Shaker* K^+ channel number and gating charge in individual *Xenopus* oocytes. *Biophys. J.* 66:A136.

Aggarwal, S., and R. MacKinnon. 1996. Contribution of the S4 segment to gating charge in the *Shaker* K^+ channel. *Neuron.* 16:1169–1177.

Armstrong, C.M., and F. Bezanilla. 1974. Charge movement associated with the opening and closing of the activation gates of Na^+ channels. *J. Gen. Physiol.* 63:533–552.

Armstrong, C.M., and F. Bezanilla. 1977. Inactivation of the sodium channel. II. Gating current experiments. *J. Gen. Physiol.* 70:567–590.

Baker, O.S., H.P. Larsson, L.M. Mannuzzu, and E.Y. Isacoff. 1998. Three transmembrane conformations and sequence-dependent displacement of the S4 domain in *Shaker* K^+ channel gating. *Neuron.* 6:1283–1294.

Baumann, A., A. Grupe, A. Ackermann, and O. Pongs. 1988. Structure of the voltage-dependent potassium channel is highly conserved from *Drosophila* to vertebrate central nervous systems. *EMBO (Eur. Mol. Biol. Organ.) J.* 7:2457–2463.

Bezanilla, F., E. Perozo, D.M. Papazian, and E. Stefani. 1991. Molecular basis of gating charge immobilization in *Shaker* potassium channels. *Science.* 254:679–683.

Bezanilla, F., E. Perozo, and E. Stefani. 1994. Gating of *Shaker* K^+ channels: II. The components of gating currents and a model of channel activation. *Biophys. J.* 66:1011–1021.

Catterall, W.A. 1988. Structure and function of voltage-sensitive ion channels. *Science.* 242:50–61.

Chen, F.S.P., D. Steele, and D. Fedida. 1997. Allosteric effects of permeating cations on gating currents during K^+ channel deactivation. *J. Gen. Physiol.* 110:87–100.

Cole, K.S., and J.W. Moore. 1960. Potassium ion current in the squid giant axon: dynamic characteristics. *Biophys. J.* 1:1–14.

Doyle, D.A., J.M Cabral, R.A. Pfuetzner, A. Kuo, J.M. Gulbis, S.L. Cohen, B.T. Chait, and R. MacKinnon. 1998. The structure of

the potassium channel: molecular basis of K^+ conduction and selectivity. *Science.* 280:69–77.

Durrell, S.R., and H.R. Guy. 1992. Atomic scale structure and functional models of voltage-gated potassium channels. *Biophys. J.* 62: 238–247.

Ellis, S.B., M.E. Williams, N.R. Ways, R. Brenner, A.H. Sharp, A.T. Leung, K.P. Campbell, E. McKenna, W.J. Koch, A. Hui, et al. 1988. Sequence and expression of mRNAs encoding the a_1 and a_2 subunits of the DHP-sensitive calcium channel. *Science.* 241: 1661–1664.

Hamill, O.P., A. Marty, B. Neher, B. Sakmann, and F.J. Sigworth. 1981. Improved patch clamp techniques for high-resolution current recording from cells and cell-free membrane patches. *Pflügers Arch.* 391:85–100.

Holmgren, M., M.E. Jurman, and G. Yellen. 1996. N-type inactivation and the S4–S5 region of the *Shaker* K^+ channel. *J. Gen. Physiol.* 108:195–206.

Hoshi, T., W.N. Zagotta, and R.W. Aldrich. 1990. Biophysical and molecular mechanisms of *Shaker* potassium channel inactivation. *Science.* 250:533–538.

Hoshi, T., W.N. Zagotta, and R.W. Aldrich. 1991. Two types of inactivation in *Shaker* K^+ channels: effects of alterations in the carboxy-terminal region. *Neuron.* 7:547–556.

Hoshi, T., W.N. Zagotta, and R.W. Aldrich. 1994. *Shaker* potassium channel gating I: transitions near the open state. *J. Gen. Physiol.* 103:249–278.

Kamb, A., L.E. Iverson and M.A. Tanouye. 1987. Molecular characterization of *Shaker*, a *Drosophila* gene that encodes a potassium channel. *Cell.* 50:405–413.

Kayano, T., M. Noda, V. Flockerzi, H. Takahashi, and S. Numa. 1988. Primary structure of rat brain sodium channel III deduced from the cDNA sequence. *FEBS Lett.* 228:187–194.

Keynes, R.D., and E. Rojas. 1974. Kinetics and steady-state properties of the charged system controlling sodium conductance in the squid giant axon. *J. Physiol. (Lond.).* 239:393–434.

Larsson, H.P., O.S. Baker, D.S. Dhillon, and E.Y. Isacoff. 1996. Transmembrane movement of the *Shaker* K^+ channel S4. *Neuron.* 16:387–397.

Liman, E.R., P. Hess, F. Weaver, and G. Koren. 1991. Voltage-sensing residues in the S4 region of a mammalian K^+ channel. *Nature.* 353:752–756.

Liu, Y., M. Holmgren, M.E. Jurman, and G. Yellen. 1997. Gated access to the pore of a voltage-dependent K^+ channel. *Neuron.* 19: 175–184.

MacKinnon, R. 1991. Determination of the subunit stoichiometry of a voltage-activated potassium channel. *Nature.* 350:232–235.

Mannuzzu, L.M., M.M. Moronne, and E.Y. Isacoff. 1996. Direct physical measure of conformational rearrangement underlying potassium channel gating. *Science.* 271:213–216.

Noda, M., T. Ikeda, T. Kayano, H. Suzuki, H. Takeshima, M. Kurasaki, H. Takahashi, and S. Numa. 1986. Existence of distinct sodium channel messenger RNAs in rat brain. *Nature.* 320:188–192.

Noda, M., S. Shimizu, T. Tanabe, T. Takai, T. Kayano, T. Ikeda, H. Takahashi, H. Nakayama, Y. Kanaoka, N. Minamino, et al. 1984. Primary structure of *Electrophorus electricus* sodium channel deduced from cDNA sequence. *Nature.* 312:121–127.

Papazian, D.M., T.L. Schwarz, B.L. Tempel, Y.N. Jan, and L.Y. Jan. 1987. Cloning of genomic and complementary DNA from *Shaker*, a putative potassium channel gene from *Drosophila. Science.* 237: 749–753.

Papazian, D.M., L.C. Timpe, Y.N. Jan, and L.Y. Jan. 1991. Alteration of voltage-dependence of *Shaker* potassium channel by mutations in the S4 sequence. *Nature.* 349:305–310.

Perozo, E., R. MacKinnon, F. Bezanilla, and E. Stefani. 1993. Gating currents from a nonconducting mutant reveal open-closed conformations in *Shaker* K^+ channels. *Neuron.* 11:353–358.

Perozo, E., L. Santacruz-Toloza, E. Stefani, F. Bezanilla, and D.M. Papazian. 1994. S4 mutations alter gating currents of *Shaker* K channels. *Biophys. J.* 66:345–354.

Perutz, M.F. 1989. Mechanisms of cooperativity and allosteric regulation in proteins. *Q. Rev. Biophys.* 22:139–236.

Pongs, O., N. Kecskemethy, R. Muller, I. Krah-Jentgens, A. Baumann, H.H. Klitz, I. Canal, S. Llamazares, and A. Ferrus. 1988. *Shaker* encodes a family of putative potassium channel proteins in the nervous system of *Drosophila. EMBO (Eur. Mol. Biol. Organ.) J.* 7:1087–1096.

Salkoff, L., A. Butler, A. Wei, N. Scavarda, K. Giffen, C. Ifune, R. Goodman, and G. Mandel. 1987. Genomic organization and deduced amino acid sequence of a putative sodium channel gene in *Drosophila. Science.* 237:744–749.

Schoppa, N.E., K. McCormack, M.A. Tanouye, and F.J. Sigworth. 1992. The size of gating charge in wild-type and mutant *Shaker* potassium channels. *Science.* 255:1712–1715.

Schoppa, N.E., and F.J. Sigworth. 1998a. Activation of *Shaker* potassium channels. I. Characterization of voltage-dependent transitions. *J. Gen. Physiol.* 111:271–294.

Schoppa, N.E., and F.J. Sigworth. 1998b. Activation of *Shaker* potassium channels. II. Kinetics of the V2 mutant channel. *J. Gen. Physiol.* 111:295–311.

Schoppa, N.E., and F.J. Sigworth. 1998c. Activation of *Shaker* potassium channels. III. An activation gating model for wild-type and V2 mutant channels. *J. Gen. Physiol.* 111:313–342.

Schneider, M.F., and W.K. Chandler. 1973. Voltage-dependent charge movement in skeletal muscle: a possible step in excitation–contraction coupling. *Nature.* 242:244–246.

Seoh, S.-A., D. Sigg, D.M. Papazian, and F. Bezanilla. 1996. Voltage-sensing residues in the S2 and S4 segments of the *Shaker* K^+ channel. *Neuron.* 16:1159–1167.

Shao, X.M., and D.M. Papazian. 1993. S4 mutations alter the single-channel gating kinetics of *Shaker* K^+ channels. *Neuron.* 11:343–352.

Sigg, D., and F. Bezanilla. 1997. Total charge movement per channel. The relation between gating charge displacement and the voltage sensitivity of activation. *J. Gen. Physiol.* 109:27–39.

Sigg, D., E. Stefani, and F. Bezanilla. 1994. Gating current noise produced by elementary transitions in *Shaker* potassium channels. *Science.* 264:578–582.

Sigworth, F.J. 1994. Voltage gating of ion channels. *Q. Rev. Biophys.* 27:1–40.

Smith-Maxwell, C.J., J.L. Ledwell, and R.W. Aldrich. 1998a. Role of the S4 in cooperativity of voltage-dependent potassium channel activation. *J. Gen. Physiol.* 111:399–420.

Smith-Maxwell, C.J., J.L. Ledwell, and R.W. Aldrich. 1998b. Uncharged S4 residues and cooperativity in voltage-dependent potassium channel activation. *J. Gen. Physiol.* 111:421–439.

Spiro, T.G., G. Smulevich, and C. Su. 1990. Probing protein structure and dynamics with resonance Raman spectroscopy: cytochrome *c* peroxidase and haemoglobin. *Biochemistry.* 29:4497–4508.

Stefani, E., L. Toro, E. Perozo, and F. Bezanilla. 1994. Gating of *Shaker* K^+ channels: I. Ionic and gating currents. *Biophys. J.* 66: 996–1010.

Stühmer, W., F. Conti, M. Stocker, O. Pongs, and S.H. Heinemann. 1991. Gating currents of inactivating and non-inactivating potassium channels expressed in *Xenopus* oocytes. *Pflügers Arch.* 418: 423–429.

Stühmer, W., F. Conti, H. Suzuki, X. Wang, M. Noda, N. Yahagi, H. Kubo, and S. Numa. 1989. Structural parts involved in activation and inactivation of the sodium channel. *Nature.* 339:597–603.

Tagliatela, M., L. Toro, and E. Stefani. 1992. Novel voltage clamp to record small, fast currents from ion channels expressed in *Xenopus* oocytes. *Biophys. J.* 61:78–82.

Tanabe, T., K.G. Beam, J.A. Powell, and S. Numa. 1988. Restoration of excitation–contraction coupling and slow calcium current in dysgenic muscle by dihydropyridine receptor complementary DNA. *Nature.* 336:134–139.

Tanabe, T., H. Takeshima, A. Mikami, V. Flockerzi, H. Takahashi, K. Kangawa, M. Kojima, H. Matsuo, T. Hirose, and S. Numa. 1987. Primary structure of the receptor for calcium channel blockers from skeletal muscle. *Nature.* 328:313–318.

Tempel, B.L., Y.N. Jan, and L.Y. Jan. 1988. Cloning of a probable potassium channel gene from mouse brain. *Nature.* 332:837–839.

Tiwari-Woodruff, S.K., C.T. Schulteis, A.F. Mock, and D.M. Papazian. 1997. Electrostatic interactions between transmembrane segments mediate folding of *Shaker* K^+ channel subunits. *Biophys. J.* 72:1489–1500.

Tytgat, J., and P. Hess. 1992. Evidence for cooperative interactions in potassium channel gating. *Nature.* 359:420–423.

Yang, N., A.L. George, Jr., and R. Horn. 1996. Molecular basis of charge movement in voltage-gated sodium channels. *Neuron.* 16: 113–122.

Yang, N., and R. Horn. 1995. Evidence for voltage-dependent S4 movement in sodium channels. *Neuron.* 15:213–218.

Yang, Y., Y. Yan, and F.J. Sigworth. 1997. How does the W434F mutation block current in *Shaker* potassium channels? *J. Gen. Physiol.* 109:779–789.

Yusaf, S.P., D. Wray, and A. Sivaprasadarao. 1996. Measurement of the movement of the S4 segment during the activation of a voltage-gated potassium channel. *Pflügers Arch.* 433:91–97.

Zagotta, W.N., T. Hoshi, and R.W. Aldrich. 1989. Gating of single *Shaker* potassium channels in *Drosophila* muscle and in *Xenopus* oocytes injected with *Shaker* mRNA. *Proc. Natl. Acad. Sci. USA.* 86: 7243–7247.

Zagotta, W.N., and R.W. Aldrich. 1990. Alterations in activation gating of single *Shaker* A-type potassium channels by the Sh^5 mutation. *J. Neurosci.* 10:1799–1810.

Zagotta, W.N., T. Hoshi, J. Dittman, and R.W. Aldrich. 1994a. *Shaker* potassium channel gating II: transitions in the activation pathway. *J. Gen. Physiol.* 103:279–319.

Zagotta, W.N., T. Hoshi, and R.W. Aldrich. 1994b. *Shaker* potassium channel gating III: evaluation of kinetic models for activation. *J. Gen. Physiol.* 103:321–362.